Earth Science Research; Vol. 11, No. 1; 2022
ISSN 1927-0542 E-ISSN 1927-0550
Published by Canadian Center of Science and Education

# Geochemistry of Volcano-sedimentary and Plutonic Formations of the Agbaou Gold Deposit, Ivory Coast

Houssou N'Guessan Nestor[1], Kouadio Fossou Jean Luc Hervé[1], Allialy Marc Ephrem[1], Kouassi Brice Roland[2] & Adingra Martial Pohn Koffi[1]

[1] University Felix HOUPHOUET-BOIGNY of Cocody-Abidjan (UFHB), UFR Earth Sciences and Mineral Resources, 22 BP 582 Abidjan 22, Côte d'Ivoire

[2] University Peleforo Gon Coulibaly Korhogo, UFR-Biological sciences, geosciences Department, Côte d'Ivoire

Correspondence: Houssou N'Guessan Nestor, University Felix HOUPHOUET-BOIGNY of Cocody-Abidjan (UFHB), UFR Earth Sciences and Mineral Resources, 22 BP 582 Abidjan 22, Côte d'Ivoire. Tel: 225-2248-3803. E-mail: nestor.houssou@gmail.com

Received: May 26, 2022 Accepted: August 3, 2022 Online Published: August 7, 2022

doi:10.5539/esr.v11n1p76 URL: https://doi.org/10.5539/esr.v11n1p76

**Abstract**

Located in the south-west part of the Fettekro greenstone belt, Agbaou gold deposit is marked by three major lithological units: (i) a volcano-plutonic unit composed of basaltic to andesitic lavas, amphibolites, chlorite-schists and sills of microdiorite and microgabbro; (ii) a volcano-sedimentary unit containing pyroclastic lavas (basaltic and dacitic) and sediments (shale and grauwacke); (iii) the late felsic dikes (rhyolite and rhyodacite) probably contemporary with the formation of granitoids form the third unit. These host rocks are mostly intensely deformed and altered. Alteration phenomena were revealed by the high values in fire loss, the decreasing of silica contents, the sometimes high values of alkaline for rocks also basic, the constant depletion in LREE and LILE. The Eu and Nb negative anomalies reveal a crustal contamination of magmatic series. Basaltic lavas are volcanic arc tholeiites nearing N-MORB type; they are associated to a magmatogenesis of ocean floor. Their magmatic source would probably be spinel lherzolitic type. Andesites have a calc-alkaline composition and seem far link to active subduction margin. Geodynamics context would be that of an area where transcurrent faults of lithospheric extension generate heat corridors able of generating by fusion the andesitic calc-alkaline magma. This context would probably be the one that prevailed during the establishment of the gold mineralization. Pyroclastic rocks of dacitic composition as acid lavas (rhyolite and rhyodacite) have also evolved in this same geotectonic context. Plutonic rocks are located in arc-volcanic granites field, while metasediment are linked to active continental margin field.

**Keywords:** Lithogeochemistry, country rocks, Birimian, Agbaou gold deposit

## 1. Introduction

West Africa is generally dominated by greenstone belts of Birimian age that are of great interest for mining research (Milési et al., 1989). These belts contain plutono-volcanic, volcaniclastic and sedimentary sequences, metamorphosed under greenschist to amphibolite facies conditions and intruded by granitoid massifs (2.2-2.0 Ga; Abouchami et al., 1990; Boher, 1991; Taylor et al., 1992; Hirdes et al., 1996; Lompo, 2010; Houssou, 2013; Houssou et al., 2014; Gnanzou, 2014; Ouattara, 2015; Houssou et al., 2017, etc.). The scarcity of fresh rock outcrops and the lack of deep work have so far prevented further investigations for an in-depth geological study of these Paleoproterozoic-aged terrains. Their geodynamic evolution remains without doubt one of the most debated subjects, the main reasons being, according to Vidal et al. (2006), the differences in structural interpretation, the lack of dating and the imprecision of the palaeogeographic reconstruction of the Palaeoproterozoic supercontinent around 1.8 Ga. Indeed, the speculations of various authors (Lemoine, 1988; Ouédraogo, 1989; Abouchami et al., 1990; Mortimer, 1990; Boher, 1991; Leake, 1992; Milési et al., 1992; Fabre et al., 1990 and 1993; Fabre and Morel, 1993; Pothin, 1993; Yao, 1993; Feybesse and Milési, 1994; Vidal and Alric, 1994; Turner, 1995; Pouclet et al., 1995; Vidal et al., 1996; Doumbia 1998; Daouda 1998; Béziat et al., 2000; Debat et al., 2003; Feybesse et al., 2006; Damparé 2008; Gueye et al., 2008; Vidal et al., 2006; Lompo 2010; etc.) are based on two main geotectonic models: (i) the so-called "modern" model emphasising collisional tectonics, crustal thickening of Archean blocks and crustal melting magmatism; and (ii) the so-called "archaic" model emphazising volume deformation and thermal phenomena related to vertical or sliding movements during the emplacement of juvenile plutons. However, features such as : the absence of inherited Archean basement (material younger than 2.4 Ga), the absence of high-grade metamorphic rocks, the absence of nappes (foliations linked to the formation of plutons or to strike-slips), the weakness of regional metamorphism (greenschist to amphibolite facies) and the absence of migmatites (except in the extreme south-west) suggest an "archaic" geodynamic evolution for the West African Craton, without however excluding the possible existence of collisional events (Vidal et al., 2006). Two major stages are noted for the creation of the Paleoproterozoic crust of the West African Craton. The first, from 2.2 Ga to 2.15 Ga in the Lower Birimian, corresponds to the formation of greenstone belts and TTG (Tonalite, Trondhjemite, Granodiorite) granitoids. The second, from 2.15 Ga to 1.9 Ga of the Upper Birimian, is characterised by the development of volcano-sedimentary basins and the production of leucogranites.

The Agbaou gold deposit, discovered in the 1980s and located in the northern region of Divo (Côte d'Ivoire), is attached to the southern part of the Fêtêkro belt. Our study, based essentially on drill cores from the Canadian company Etruscan Resources (now Endeavour Mining), is intended to contribute to the improvement of our knowledge of the Birimian formations. This work will focus on the lithogeochemical study of the country rocks to chemically characterize these formations and to determine their geotectonic environment of emplacement.

## 2. Geological Context

The Agbaou gold deposit is located in the southern part of the Oumé-Fètèkro Birimian belt, which is part of the Proterozoic domain of Côte d'Ivoire. This part belongs to the Man Ridge in the West African Craton (Figure. 1A). Indeed, the Proterozoic domain was structured during orogenies. This framework is still the subject of debate because, for some authors (Tagini, 1971; Yacé, 1993), it took place during a single orogeny, the Eburnean (2500-1600 Ma), for others (Lemoine, 1988; Boher, 1991) this structuring took place during two orogenesis, the Burkinian (2400-2150 Ma) and the Eburnean (s.s.) (2120-1800 Ma). Papon (1973) proposes a subdivision of Proterozoic domain into two distinct zones: (i) the SASCA type-(Sassandra-Cavally) zone located in south-west of the country, where the Archean formations are well preserved and (ii) the geosynclinal-type, which occupies the rest of the domain. The formations of this second zone are attributed to the Birimian (Arnould, 1961; Bonhomme, 1962). They are consisting of sedimentary and volcanic-plutonic belts generally oriented NE-SW, and separated by oriented or equant granitoids. The works of Yacé (1982), Lemoine (1988), Olson (1989), Mortimer (1990), Leake (1992), Daouda (1998), Ouattara et al. (2008), Houssou et al. (2011), Houssou (2013), Allou (2014), Ouattara (2015), Houssou et al. (2017), Coulibaly (2018), have provided details on both geological setting of the Oume-Fetekro belt and the gold mineralisations of Bonikro, Agbaou and Bobosso.

The geology of the Agbaou deposit, the subject of our study, is defined by two major lithological units of Birimian age crossed by vein formations: (i) a mafic to intermediate volcanic unit consist of basalt and andesite and (ii) a volcano-sedimentary unit (Figure. 1B). This second unit includes tuff-type pyroclastics, sandstones, siltstones and mudstones. These birimian formations are generally deformed and metamorphosed in the greenschist to amphibolite facies. They outcrop in the form of metabasalts, meta-andesites, schists (chloritoschists, calco-chloritoschists and sericitoschists), amphibolites, mylonites and breccias. These different rocks have undergone significant deformation, the extent of which has been revealed by geophysical data (Gillick, 2001), remote sensing (Houssou, 2013), drill cores (Houssou, 2013) and the mine pits. These data suggest the existence of a regional tectonic subparallel to the NE birimian direction and major faults or shear zones. The NE faults correspond to shear zones including the Agbaou Tectonic Zone (ATZ) and the West Tectonic Zone (WTZ). The ATZ is practically a first order megastructure, which is estimated to be about 500 meters wide and 2 kilometers long (Tourigny, 2008). The NW dislocations, which appear to be more recent, simply intersect or sometimes offset earlier structures. Gold mineralization is controlled by shear zones that host mineralized lenses with associated quartz vein networks.

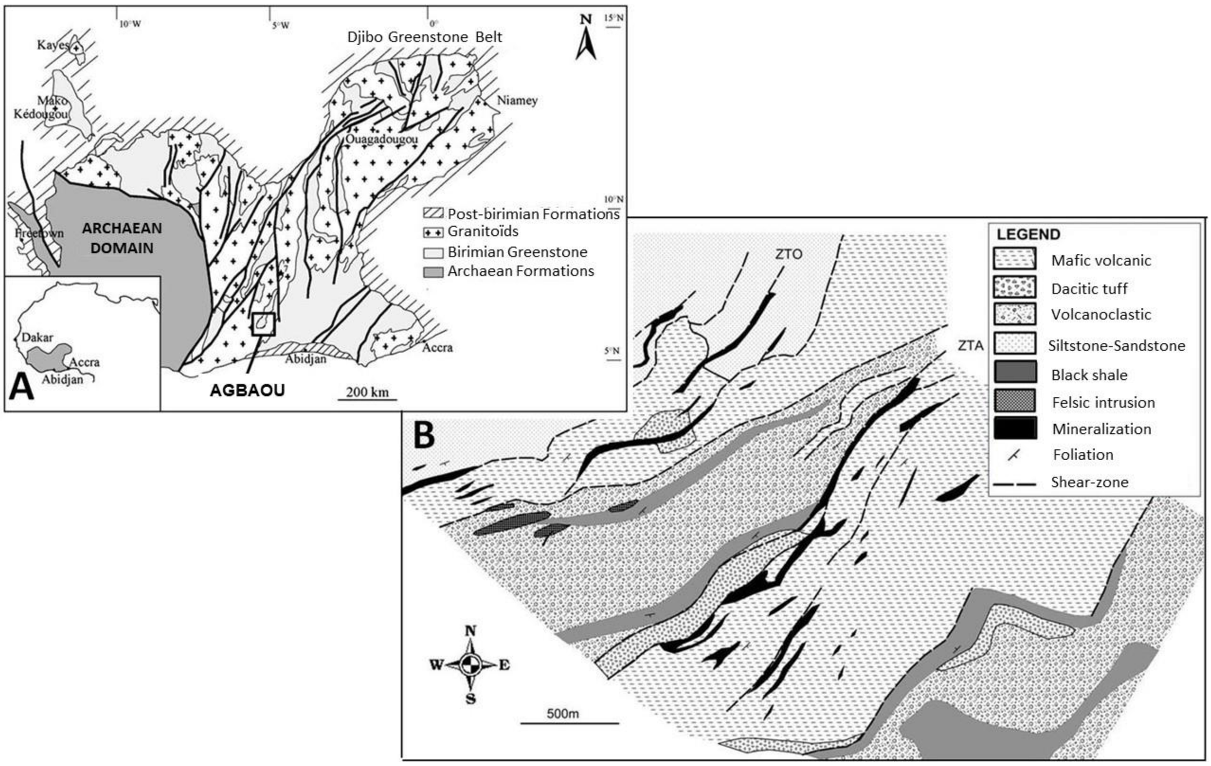


Figure 1. (A) Simplified geological map of the West African craton and location of the Agbaou gold deposit (map redrawn from Milesi et al., 1992). (B) Lithostructural map of the Agbaou mine

## 3. Material and Methods

Thirty samples of the host rocks were chemically analyzed. These samples were crushed and then porphyrized in an Agathe bowl at the Chemical Laboratory of SODEMI (Société pour le Développement Minier de Côte d'Ivoire). The powder obtained was then analysed at the Service d'Analyse des Roches et des Minéraux (SARM) of the Centre de Recherche Pétrographique et Géochimique (CRPG) in Nancy, France. Major elements were determined by plasma emission spectrometry (ICP). Trace elements were analysed by inductively coupled plasma-mass spectrometry (ICP-MS)

## 4. Results

### *4.1 Major and Trace Elements Composition*

**a. Metasediments**

The petrographic study showed that the Agbaou metasediments are mostly sericite schists. Sericite is generally related to the pseudomorphosis of feldspars, an abundant mineral in the sediments. The metasediments show concentrations of 58.17 and 66.14 % SiO2, 4.44 and 7.80 % alkalis ($Na_2O$ + $K_2O$), 15.35 and 15.80 % $Al_2O_3$ and 0.61 and 0.89 % $TiO_2$. MgO contents are low (1.85 and 2.27%). The geochemical criteria commonly used for the classification of sediments are $SiO_2$ concentrations, with $SiO_2/Al_2O_3$ ratio (Potter, 1978) which reflecting the abundance of quartz and the content of clays and feldspars. The other criteria used is the alkali content ($Na_2O$ + $K_2O$); this seems less relevant here for establishing the classification, given the phenomena of metamorphism and alteration. Based on the chemical maturity index and the $Fe_2O_3$ /$K_2O$ ratio, Herron (1988) proposed a classification of terrigenous sediments based on the log ($SiO_2/Al_2O_3$)-log ($Fe_2O_3$ /$K_2O$) diagram. He modified the diagram established by Pettijohn et al (1972), replacing log ($Na_2O$ + $K_2O$) by log ($Fe_2O_3$ /$K_2O$). The log ($SiO_2/Al_2O_3$)-log ($Fe_2O_3$ /$K_2O$) diagram shows that the Agbaou metasediments correspond to greywackes and shales (Figure 2A). Chromium, cobalt, nickel and vanadium compositions are generally higher in shales than in grauwackes. The shales have Cr, Co, Ni and V contents of 114 ppm, 51 ppm, 56 ppm and 187 ppm respectively; these values are respectively 59 ppm, 14 ppm, 22 ppm and 84 ppm in the greywackes.

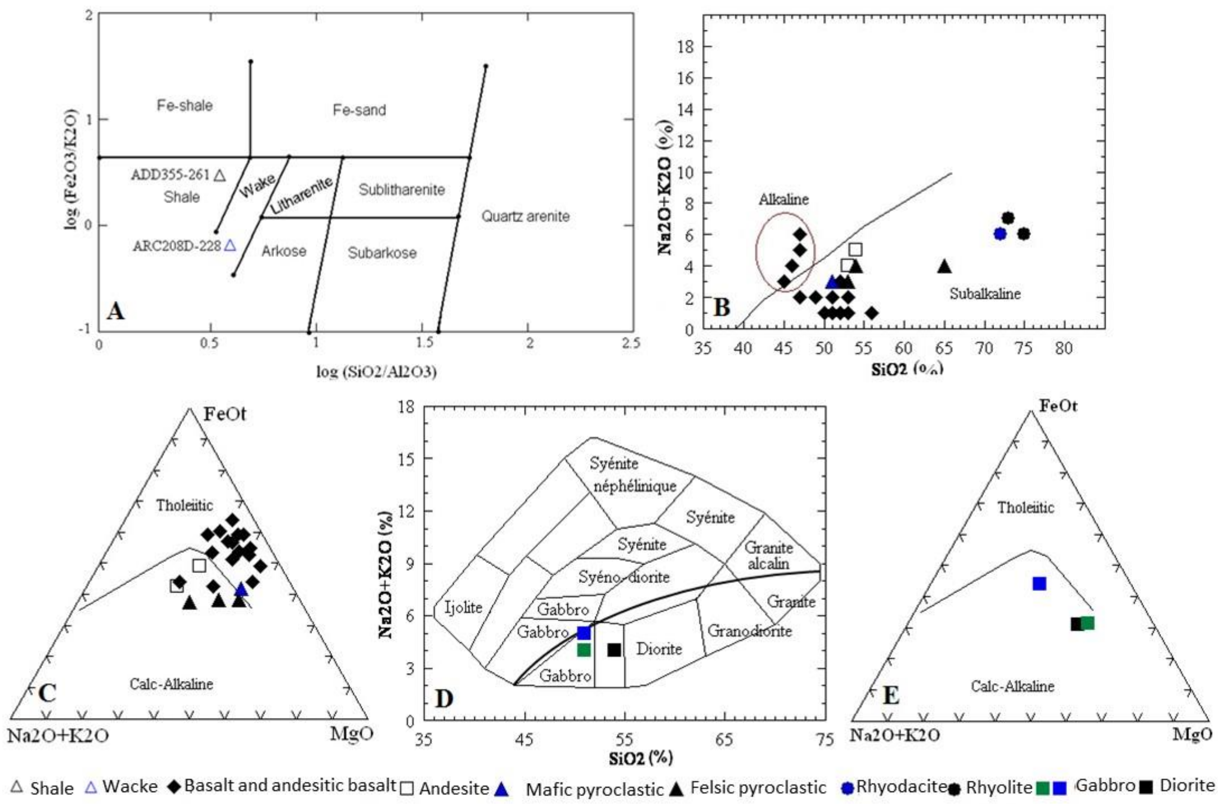


Figure 2. (A) Log (SiO2/Al2O3)-log (Na2O/K2O) discrimination diagram by Herron (1988) applied to sediments; (B) SiO2 versus Na2O + K2O diagram (Irvine and Baragar, 1971) applied to metavolcanites; (C) AFM diagram (Irvine and Baragar, 1971) applied to metavolcanites; (D) SiO2 versus Na2O + K2O diagram (Cox et al., 1979) adapted to plutonic rocks by Wilson (1989) applied to plutonites; (E) AFM diagram (Irvine and Baragar, 1971) applied to metaplutonites from the Agbaou deposit

The trace element compositions of the metasediments are plotted on multi-element diagrams normalized to the upper continental crust (Figure 3A), basing on the values of Taylor and McLennan (1985). The profiles are generally flat and marked by depletions of lithophile ions LILE and HFSE (U, Th, Nb and Ta). There is a relative deficit in Zr compared to elements with a similar degree of compatibility. The greywackes show strong positive anomalies in Rb and Ba. The fractionation of the sediments is characterized by element ratios of the radioactive / radiogenic pairs: Rb/Sr (0.15-0.38) and Sm/Nd (0.21); these values are close to the values (0.32 and 0.17, respectively) estimated for the upper continental crust (Taylor and McLennan, 1985).

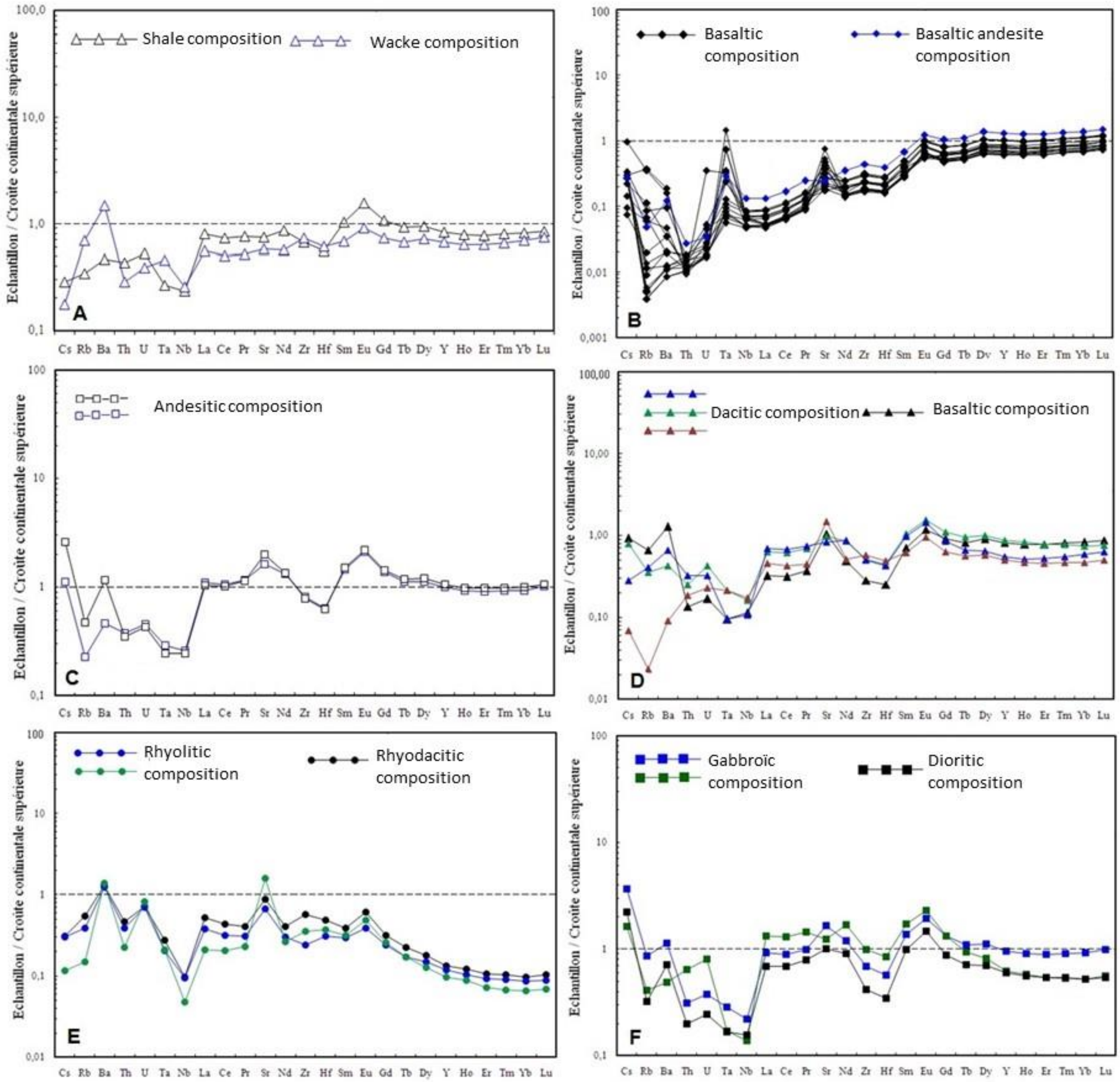


Figure 3. Spidergrams of metasediments (A), basalts and basaltic andesites (B), andesites (C), pyroclastites (D), felsites (E) and plutonites (F) from the Agbaou deposit normalized to the upper continental crust

**b. Metavolcanites**

The concentrations of $SiO_2$ and alkalis ($Na_2O + K_2O$) indicate that the volcanics have a composition of basalt and basaltic andesite, andesite, dacite, rhyolite and rhyodacite. The volcanics are generally subalkaline, except for those in mineralized areas which are mostly alkaline character (Irvine and Baragar, 1971; Figure 2B). Basalts and basaltic andesites are the dominant lithology of the metavolcanites. They are characterized by $SiO_2$ contents from 45.28% to 56.18%, alkalis ($Na_2O + K_2O$) from 1.08% to 6.63%, $Al_2O_3$ from 12.04% to 16.84% and TiO2 (0.63-1.71%). MgO values range from 5.35 to 9.44%. These formations are generally tholeiitic composition (Irvine and Baragar, 1971; Figure. 2C). However, they are weakly potassic. The rocks in the mineralized zones show a rather alkaline character and very low $SiO_2$ contents. Metal concentrations in basalts and basaltic andesites are: chromium (108-375 ppm), cobalt (39-52 ppm), nickel (73-178 ppm) and vanadium (215-374 ppm). The trace element compositions for basalts and basaltic andesites are plotted on diagrams normalized to upper continental crust (Figure. 3B), basing on the values of Taylor and McLennan (1985). The patterns of these rocks show a general trend of depletion for incompatible elements expressed by the slope in the diagrams. However, the relatively high Ta and Sr contents, compared to elements with a close degree of incompatibility are expressed by positive anomalies. There is a relative deficit in Rb. The fractionation is marked by very low (0-0.28) and high (0.33-0.37) Rb/Sr and Sm/Nd element ratios compared to the values (0.32 and 0.17, respectively) estimated (Taylor and McLennan, 1985) for the upper continental crust.

The andesites have undergone the effects of epizonal metamorphism and alteration. They are defined by contents of 53.16-54.20% SiO2, 4.65-6.11% alkali ($Na_2O$ + $K_2O$), 4.18-5.52% MgO, and low $TiO_2$ values 0.93-0.99%. They have a basaltic andesite composition (Figure. 2B). The andesites are calc-alkaline and weakly to moderately potassic (Figure. 2C). These rocks have average vanadium contents between 171 and 205 ppm. Chromium, cobalt and nickel contents are low and are respectively between 36-65 ppm, 27-35 ppm and 41-72 ppm. The Agbaou andesites show lower Cr, Co and Ni contents than the Ashanti andesites: Cr (160-270 ppm), Co (30-48 ppm) and Ni (40-120 ppm); however, their V contents are similar (105-202 ppm).

The trace elements composition of the andesites is shown in diagrams normalized to upper continental crust (Figure. 3C), according to the values of Taylor and McLennan (1985). The profiles are relatively flat and generally show a depletion of lithophile ions LILEs (Rb, Ba) and HFSEs (Th, U, Ta, Nb and Hf). This very marked negative anomaly in Nb is characteristic of the continental crust; There are strong positive anomalies in Sr, Cs and Eu. The fractionation is marked by ratios of radioactive / radiogenic elements: Rb/Sr low (0.04-0.08) and Sm/Nd identical (0.19-0.20) compared to the values (0.32 and 0.17, respectively) estimated for the upper continental crust (Taylor and McLennan, 1985).

The pyroclastics are either basaltic or dacitic in composition (Figure. 2B). They are indeed quartz vein walls, which have undergone the effects of alteration; this is revealed by their very high loss on ignition values (>10%). There is a strong remobilization of silica. The basaltic pyroclastics correspond to the mafic pyroclastics described in the petrographic study above. They have $SiO_2$ contents of 51.69% and alkaline contents ($Na_2O$ + $K_2O$) of 4.07%. These pyroclastites are very magnesian with MgO = 9.41 %; they show low TiO2 contents (0.89 %). They straddle the tholeiitic and calc-alkaline series (Figure. 2C) and are highly potassic. The dacitic pyroclastites, on the other hand, correspond to the felsic pyroclastites as also described in the petrographic study paragraph. Their $SiO_2$ values are between 53.41-65.15% and alkali ($Na_2O$ + $K_2O$) between 3.48-5.05%. MgO contents vary from 4.46% to 8.08%. These acid pyroclastites are linked to the calc-alkaline series (Figure. 2C) and are moderately potassic. The Agbaou pyroclastites have progressively decreasing metal contents in the following order: chromium, cobalt, nickel and vanadium. The basaltic pyroclastites have high chromium contents (513 ppm) followed by vanadium (244 ppm), nickel (97 ppm) and cobalt (38 ppm). The same is true of the dacitic pyroclastics which have very expressive chromium contents (329-518 ppm), followed by vanadium (84-206 ppm), nickel (72-138 ppm) and cobalt (24-31 ppm).

Their incompatible element compositions are highlighted in multi-element diagrams normalized to the upper continental crust (Figure. 3D), basing on the values of Taylor and McLennan (1985). Overall, the patterns of the pyroclastites are flat and show depletions in light lithophile ions LILE and HFSE (Zr, Hf, Nb and Ta). The typical dacitic pyroclastite, which offers the strongest deficit in Cs, Ba and Rb, shows a positive anomaly in Sr which has the highest Cs, Ba and Rb deficiency, shows a positive Sr anomaly. The basaltic pyroclastite also shows a positive Sr anomaly. The fractionation is marked by low Rb/Sr (0.01-0.20) and Sm/Nd (0.20-0.25) ratios, identical to the values (0.32 and 0.17, respectively) estimated for the upper continental crust (Taylor and McLennan, 1985).

The acidic lavas are mostly rhyolites and rhyodacites (Figure 2B). They are supersaturated and generally consist of feldspar and quartz phenocrysts with crystallization gaps. Rhyodacites also contain more or less chloritized biotite phenocrysts. They have $SiO_2$ of 72.13% and alkaline ($Na_2O$ + $K_2O$) of 7.21% contents. Their MgO content is low (0.73%), as is TiO2 (0.29%). The rhyolites, on the other hand, are characterized by SiO2 values of 73.30% to 75.97% and alkalis ($Na_2O$ + $K_2O$) of 7.06% to 7.70%. The MgO and $TiO_2$ contents are very low and give respectively 0.10-0.45% and 0.05-0.14%. At Agbaou, these acid intrusions are late and crosscut all the volcano-sedimentary units without exposing any particular phenomena of contact metamorphism. They contain low levels of chromium (41-85 ppm), cobalt (0-4 ppm), nickel (0-9 ppm) and vanadium (1-24 ppm). Radioactive element values are also relatively low: U (1.97-2.31 ppm) and Th (2.42-5.00 ppm). The trace element compositions of the acid intrusions are plotted on diagrams normalized to upper continental crust (Figure. 3E), according to the values of Taylor and McLennan (1985). The patterns are generally shallowly sloping and marked by depletion of HFSE-bearing elements. Relatively low Nb contents compared to elements with a similar degree of incompatibility are expressed by negative anomalies on the diagrams similar incompatibility are expressed as negative anomalies on the diagrams. Strong positive anomalies in Sr and Ba are also noted. The Zr/Y (17-37) and La/Yb (43-74) ratios appear to be relatively high. The fractionation of the lavas is marked by element ratios of the radioactive / radiogenic pairs: Rb/Sr very low (0.03-0.19) and Sm/Nd identical (0.17-0.21) compared to the values (0.32 and 0.17, respectively) estimated for the upper continental crust (Taylor and

McLennan, 1985).

**c. Metaplutonites**

The classification diagram of Cox et al. (1979), adapted to plutonic rocks by Wilson (1989), shows that the metaplutonites of Agbaou deposit have a composition of diorite and gabbro (Figure 2D). The petrographic study revealed that they are microdiorites and microgabbros. These rocks are essentially subalkaline. The diorites have a $SiO_2$ content of 54.62% and alkaline ($Na_2O$ + $K_2O$) of 5.69%. Their MgO content is very high (9.06%). The $TiO_2$ content is low (0.67%). The diorites belong to the calc-alkaline series (Figure 2E). The gabbros have $SiO_2$ concentrations from 51.27% to 51.39% and alkaline ($Na_2O$ + $K_2O$) from 30% to 6.05%. Their MgO values are high (6.08-11.70%). TiO2 contents are low (0.67-0.95%). The gabbros also belong to the calc-alkaline series (Figure 49E). The plutonites are marked by identical cobalt concentrations (diorites: 41 ppm and gabbros: 32-41 ppm), the differences being in chromium, vanadium and nickel. The diorites show Cr (590 ppm), V (157 ppm) and Ni (277 ppm) while the contents in the gabbros are: Cr (65-453 ppm), V (141-218 ppm) and Ni (96-208 ppm).

The trace element compositions of the metaplutonites are plotted on multi-element diagrams normalized to the upper continental crust (Figure. 3F), according to the values of Taylor and McLennan (1985). The profiles are relatively flat with depletions in LILE (Rb and Ba) and HFSE (Nb, Ta, Hf and Zr). There are enrichments in Cs. The element ratios of the radioactive / radiogenic pairs give low Rb/Sr (0.10-0.16) and identical Sm/Nd (0.17-0.20) compared to the values (0.32 and 0.17, respectively) estimated for the upper continental crust (Taylor and McLennan, 1985).

*4.2 Rare Earth Composition*

**a. Metasediments**

The rare earth compositions (ΣREE) of the Agbaou metasediments are respectively 117.58 ppm and 80.51 ppm. These concentrations plotted on chondrite-normalized diagrams, according to Sun and McDonough (1989) (Figure. 4A), show similar, low-slope rare earth spectra with low fractionation rates: (La/Sm) N = 3.27-3.43 and (La/Yb) N = 7.48-9.10. However, the grauwackes show a weak negative europium anomaly.

**b. Metavolcanites**

Rare earth concentrations (ΣREE) in basalts and basaltic andesites are low and range from 19.88 to 47.03 ppm. Plotted on chondrite-normalized diagrams (Sun and McDonough, 1989; Figure. 4B), the rare-earth spectra are relatively flat with very little fractionation: $(La/Sm)_N$ = 0.65-0.82 and $(La/Yb)_N$ = 0.56-0.90. Basaltic andesites show relatively higher rare earth contents than basalts. However, there is a slight general depletion of LREE. The basaltic rocks of Agbaou show negative europium anomalies (Eu/Eu* = 1.36) and thus develop a geochemical behavior similar to that of N-MORB basalts.

The rare earth compositions (ΣREE) of the andesites of Agbaou are very high and range from 163.81 to 165.79 ppm. These concentrations plotted on chondrite-normalized diagrams (Sun and McDonough, 1989; Figure. 4C), indicate moderately sloping rare-earth spectra with a low fractionation rate: $(La/Sm)_N$ = 2.88-3.13 and $(La/Yb)_N$ = 9.60-10.76. The rare earth contents of the andesites are in the order of 8 to 100 times the chondrite. There is absence of europium anomalies.

Rare earth contents (ΣREE) are around 60.85 ppm in basaltic pyroclastites and 68.87 ppm in dacitic pyroclastites. The pyroclastites which are mostly wall hangings of mineralized quartz veins showing higher rare earth contents (163-165 ppm). The rare earth compositions of the pyroclastites are plotted on chondrite-normalized diagrams (Figure. 4D) according to the values of Sun and McDonough (1989). The rare earth spectra of pyroclastites are generally low to medium slope. Basaltic pyroclastites show very low fractionation [$(La/Sm)_N$ = 1.89 and $(La/Yb)_N$ = 3.59], lower than ~~that~~ of dacitic pyroclastites [$(La/Sm)_N$ = 2.57-3.16 and $(La/Yb)_N$ = 7.91-10.87]. There is no europium anomaly.

The rare earth contents (ΣREE) of rhyodacites are around 61.31 ppm, while those of rhyolites range from 31.44 to 45.50 ppm. Spectra of acid lavas normalized to chondrite composition (Sun and McDonough, 1989; Figure. 4E), show generally steep slopes. The fractionation rate of rhyolites is: $(La/Sm)_N$ = 2.74-5.62 and $(La/Yb)_N$ = 29.42-50.10. A slight general depletion of Sm is noted.

**c. Metaplutonites**

The rare earth contents (ΣREE) of diorites are 108.84 ppm, while those of gabbros are higher and range from 145 to 197.30 ppm. The rare earth spectra of plutonites normalized to chondrite values (Sun and McDonough, 1989; Figure. 4F), are moderately to steeply sloping. Diorites and gabbros show similar spectra although the rare earth contents of the latter appear to be higher. Their fractionation rates are also close and relatively low: Diorite [$(La/Sm)_N$ = 2.94 and $(La/Yb)_N$ = 12.11] and Gabbro [$(La/Sm)_N$ = 2.80 and $(La/Yb)_N$ = 9.12]. However, a gabbro sample gave a higher fractionation rate of: $(La/Sm)_N$ = 3.26 and $(La/Yb)_N$ = 23.29.

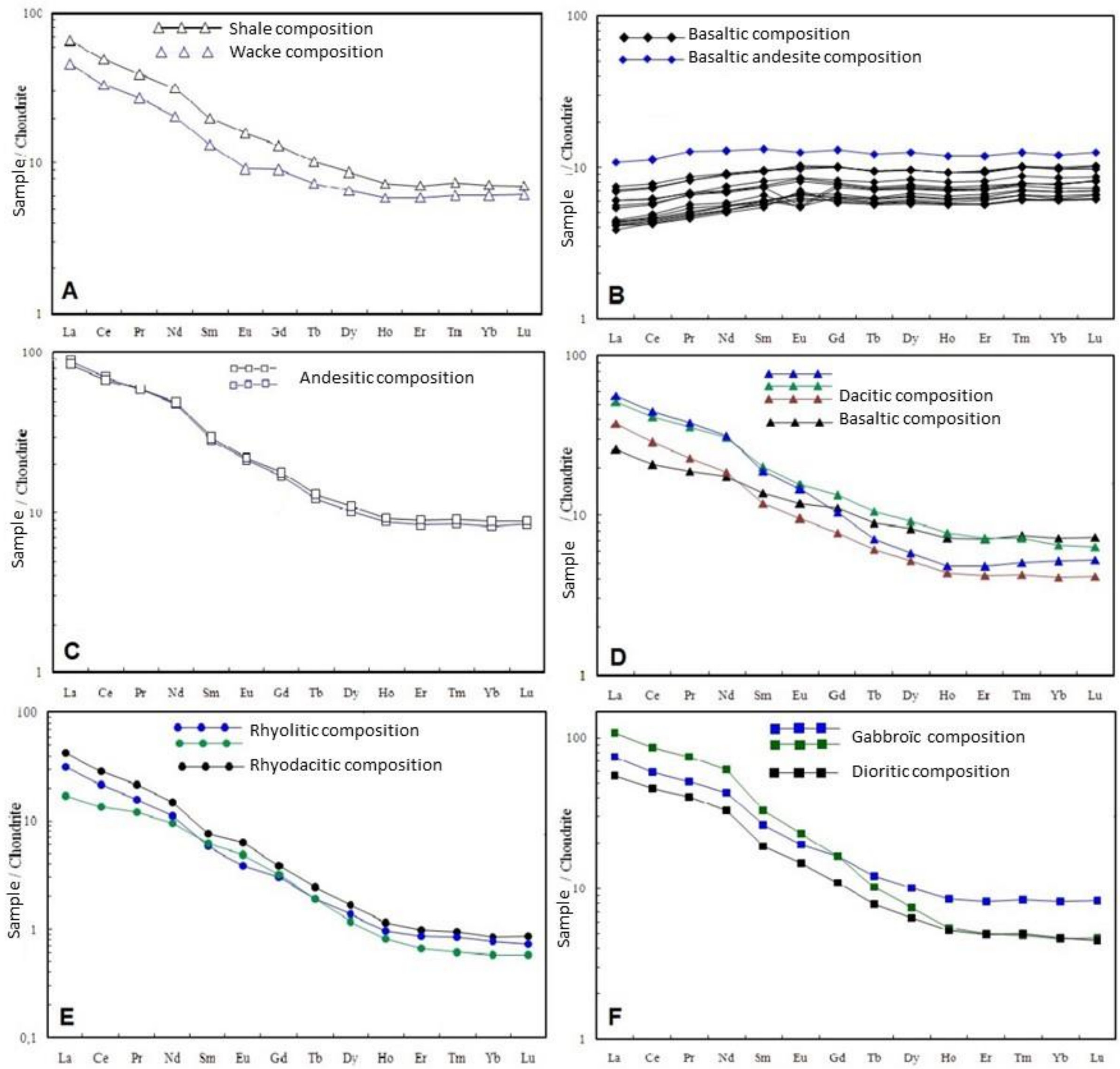


Figure 4. Rare earth spectra of metasediments (A), basalts and basaltic andesites (B), andesites (C), pyroclastites (D), felsites (E), plutonites (F) from the Agbaou deposit normalized to chondrite

### 5. Petrogenesis and Geotectonic Relationships

#### a. Metasediments

Agbaou sediments are plotted in the field of active continental margins on the log ($K_2O/Na_2O$) versus $SiO_2$ discrimination diagram of Roser and Korsch (1986) (Figure. 5A). The rare earth fractionation rate of these sediments is generally low, with a well-expressed positive Eu anomaly. The low Cr content can be explained by the fact that Cr was mobilized during the diagenesis process that seems to be at the origin of the sedimentary rocks. Only the greywacke shows a strong positive anomaly in Rb and Ba. The positive Eu anomalies imply crystallization of plagioclases and alkali feldspars by fractional crystallization or partial melting of the rock.

#### b. Metavolcanites

The basalts and basaltic andesites of Agbaou, compared to the lavas of classical geodynamic contexts, show geochemical signatures close to N-MORB basalts marked by a depletion of large lithophile ions (LILEs) on spiderdiagrams normalized to the upper continental crust. However, the Agbaou lavas are characterized by very marked Ta anomalies and higher Cs contents. The Nb/Yb-Th/Yb diagram (Figure. 5B) confirms this affinity of the Agbaou basaltic rocks to N-MORB basalts and suggests a depleted magmatic source, intermediate between E-MORB and N-MORB. They are also marked by low Th/Nb ratios (0.07-0.10). These low Th/Yb values (0.07-0.10) are indicative of subduction or low crustal contamination.

The andesites, on the other hand, correspond to intraplate formations (Within-Plate Basalt, WPB) with a calc-alkaline composition (Calc-Alkaline Basalt, CAB) (Figure. 5B). They have a relatively high Th/Nb ratio (0.62) compared to basalts and basaltic andesites and to the mantle. Indeed, the mantle shows a constant Th/Nb ratio expressed by a linear correlation between Th/Yb and Nb/Yb. There was therefore probably crustal contamination of these formations. The andesites are also marked by a high Th/Yb ratio (1.72-1.96) compared to the basaltic rocks (0.07-0.10); this implies that the andesites, during their evolution, were affected by a crustal contamination.

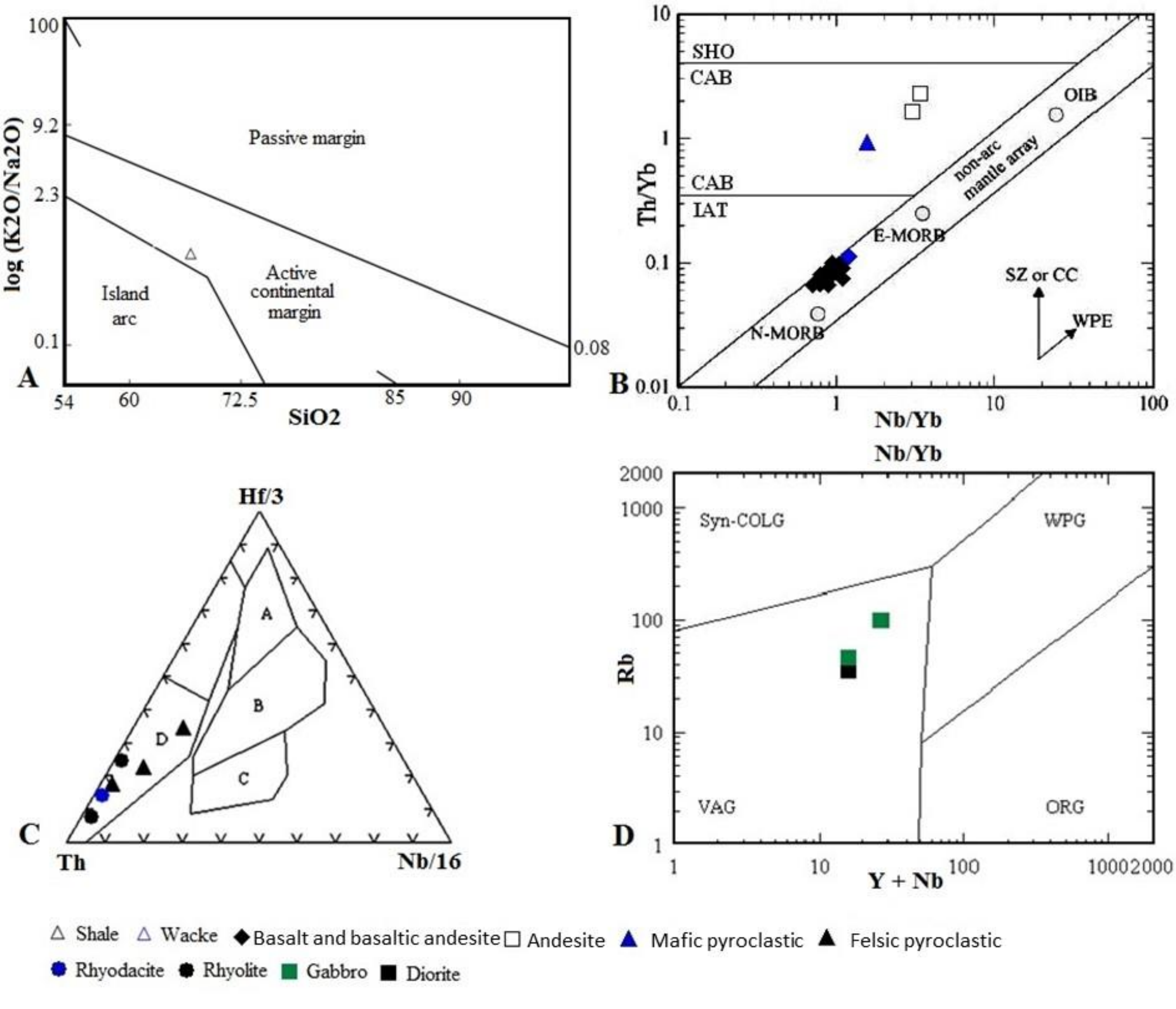


Figure 5. Petrogenetic diagrams of volcanosediments and plutonites

(A) SiO2-log (K2O/Na2O) discrimination diagram of Roser and Korsch (1986) applied to sediments; (B) Pearce (1983) Nb/Yb-Th/Yb diagram applied to the metavolcanites of the Agbaou deposit, illustrating Th enrichment in the subduction zone or crustal contamination. SZ: Subduction zone flow. IAT: Island arc tholeiites. CAB: Calc-alkaline basalts. SHO: Shoshonitic basalts. N-MORB, E-MORB and OIB (after Sun and McDonough, 1989). (C) Th-Nb-Hf discrimination diagram of Wood (1980) applied to metavolcanites; A: N-MORB; B: E-MORB and intraplate tholeiites; C: alkaline intraplate basalts; D: volcanic arc basalts. (D) Y+Nb-Rb discrimination diagram of Pearce et al (1984) applied to Agbaou plutonites. Syn-COLG: syn-collisional granites; WGP: intraplate granites; VAG: volcanic arc granites; ORG: oceanic rift granites.

The mafic pyroclastites show geochemical characteristics similar to those of basaltic rocks; they correspond to N-MORB (Figure. 5B). These pyroclastites have a relatively high Th/Nb ratio (0.51). They may have undergone moderate crustal contamination (Th/Yb = 0.80). Dacitic pyroclastics, on the other hand, correspond to arc volcanics (Figure. 5C) and seem to have evolved in the same geotectonic context as the acid lavas.

The acid dykes, formed by rhyolites and rhyodacites, are set in the field of the arc volcanics (Figure. 5C). The rhyolites have low Y concentrations (Y<5ppm) and high Zr/Y concentrations (Zr/Y>10), showing that they belong to the FI rhyolites (Lesher et al., 1986).

**c. Metaplutonites**

Chemical analyses of the metaplutonites are shown in the (Y + Nb) versus Rb diagram of Pearce et al. (1984) (Figure. 5D). It is clear that the diorites and gabbros are close to the volcanic arc plutonites (VAG). The plutonites of the Agbaou deposit show significant depletion of high potential elements (HFSE) (Nb, Ta, Zr and Hf), low HREE and very strong positive Eu anomalies.

**6. Discussion**

Geochemical data reveal that the volcanics of the Agbaou gold deposit have compositions of basalt and basaltic andesite, andesite, dacite, rhyodacite and rhyolite. These volcanics are subalkaline, except for those in the mineralized zones which character are rather alkaline. Sedimentary units (sandstones, shales and greywackes) are associated with these volcanics; the whole being intruded by microdiorites and microgabbros, but also by late felsite dikes (rhyolites and rhyodacites).

The Agbaou volcanics have very low $TiO_2$ contents ranging from 0.05-1.71%. This suggests that these are similar to magmatic arc volcanics (Pearce and Cann, 1973), but distinct from those of intraplate volcanism which have higher $TiO_2$ contents (>2%). The basaltic lavas of Agbaou consistently exhibit flat rare earth spectra with low LREEs depletion and low Ce contents. They show geochemical characteristics similar to those described by Daouda (1998) in the basalts of the Toumodi area located further north but also belonging to the Fêtêkro belt. The Agbaou basalts have relatively lower Cr, Co, Ni and V contents than their counterparts in the Ashanti belt, Ghana (Dampare et al., 2008). On the one hand, identical Ni contents are noted in the basalts and andesites of Agbaou, and on the other hand, a decrease in Cr, Co and V contents from basalts to andesites. There is also a generalized depletion of large lithophilic ions (LLIs) in basaltic rocks. Indeed, the content of light and more mobile elements characteristic of the continental crust suggests a crustal contamination of the magmas. The Sr enrichment is indicative of the presence of plagioclase in the Agbaou basalts. Normative compositions indicate the presence of olivine in basaltic rocks. However, this mineral was not observed in our fresh rocks during the petrographic study. Indeed, olivine has an essentially magmatic origin. It must therefore have been transformed into tremolite during hydrothermal alteration. Tremolite was indeed observed in the rock during the petrographic study. To this must be added the positive anomaly in Ta, probably indicating the presence of ilmenite, rutile or sphene in the Agbaou metabasalts. The basaltic lavas correspond to arc-volcanic tholeiites close to N-MORB, as suggested by various authors on the Man-Léo Ridge lavas (Abouchami et al., 1990; Mortimer, 1990; Boher et al., 1992; Leake, 1992; Daouda, 1998; Lompo, 2009; etc.). They have been dated to 2.5-1.5 Ga and their magmatic source is thought to be spinel lherzolite. These lavas are probably related to an oceanic plateau-type magmatogenesis. MORB basalts are generally interpreted as being formed from a mantle depleted in elements incompatible with liquidus temperatures of 1200 ℃ and represent an extension of mid-ocean ripples or back-arc basins. Unlike the basalts of the Agbaou gold deposit, which are tholeiitic in character, the basalts of the Sabodala gold deposit (in eastern Senegal) correspond to type A basalts with a komatiitic tendency (Sylla and Ngom, 1997). The andesites are characterized by moderate fractionation of light rare earths, negative Eu and Nb anomalies, and moderate enrichment in LILEs (Cs, Ba and Rb). The Nb anomaly associated with an enrichment in light lithophilic ions suggests a crustal involvement in magmatism. The Agbaou andesites have a calc-alkaline composition and seem to be related to an active margin subduction context. Indeed, calc-alkaline magmas are classically associated with an active margin subduction context. However, for the Fêtêkro Birimian belt, very few authors argue in favor of a subduction zone, except Lemoine (1988) and Mortimer (1990). The former proposes a subduction model with crustal delamination, while the latter thinks rather of a birimian magmatism linked to a collision model with subduction. Indeed, the metamorphism at Agbaou is of low grade and greenschist facies; it only reaches amphibolite facies at the level of the shear corridor. Consequently, linking the geodynamic evolution of the Agbaou gold deposit to a subduction zone becomes problematic. The geotectonic context would be that of a zone where transcurrent lithospheric extension faults by friction generate thermal corridors capable of generating andesitic calc-alkaline magma by melting.

The pyroclastites are located in the field of volcanic arc basalts and appear to be related to calc-alkaline magmatism. Geochemical analyses have also shown that the sediments correspond to shales and greywackes emplaced in an active continental margin type geodynamic environment such as in the Comoé Basin (Adingra et al., 2018) and in the Sassandra-Cavally (SASCA) domain (Koffi et al., 2018).

The Agbaou metaplutonites, formed of diorites and gabbros, correspond to volcanic arc plutonites. The strong depletion of HFSEs, weak depletion of HREEs and strong positive europium anomalies suggest that the metaplutonites are probably related to calc-alkaline magmatism of active margins.

Concerning the acid lavas, they are composed of rhyodacite and rhyolite. They are marked on the one hand by depletion of HFSEs and HREEs and on the other hand by negative Nb and positive Eu and Sr anomalies. Geochemical data indicate that the acid lavas correspond to arc volcanics, with an M-type affinity. The low Y and high Zr/Y values suggest that rhyolites and rhyodacites of Agbaou deposit are close to FI or Fill felsic metavolcanics rocks type I as defined by Lesher et al. (1986). Indeed, these felsites are generally interpreted as being formed by low-temperature (<900 °C) melts at deep levels in the crust (>10 km) (Lesher et al., 1986; Hart et al., 2004). According to these authors, these melts have low potential to drive hydrothermal systems due to their low melting temperature and heat loss during transport to the surface of the Earth's crust.

## 7. Conclusion

The host rocks of the Agbaou deposit are mostly deformed and altered. The alteration phenomena were revealed by the high values of loss on ignition (LOI), the reduction of silica ($SiO_2$) contents, the sometimes-high alkali values for such basic rocks, the constant depletion of light rare earths LREE and large lithophile ions LILE (Cs, Rb, Ba, etc.). The negative Eu and Nb anomalies are indicative of crustal contamination of the magmatic series.

The binary and ternary diagrams made it possible to classify the host rocks of the Agbaou deposit into basalts and basaltic andesites, andesites, basaltic and dacitic pyroclastics, rhyodacites and rhyolites (dykes), diorites and gabbros (sills) and, finally, sediments formed by greywackes and shales.

The basalts and basaltic andesites of Agbaou exhibit flat rare earth spectra with low enrichments of LREEs. Low Ce and Ti contents are also noted. These basaltic rocks are similar to the N-MORBs and are related to an oceanic plateau type magmatogenesis. Their magmatic source is probably spinel lherzolite. The andesites have a calc-alkaline composition and seem to be related to an active margin subduction context. On the contrary, their tectonic context would be that of a zone where transcurrent lithospheric extension faults by friction generate thermal corridors capable of generating calc-alkaline andesitic magma by melting. This context would undoubtedly be the one that prevailed in the setting of the Agbaou gold mineralization. Dacitic pyroclastics and acid lavas also evolved in this same geotectonic context. The metaplutonites are located in the field of arc-volcanic granites. The metasediments, on the other hand, are located in the field of an active continental margin.

## References

Abouchami, W., Boher, M., Michard, A., & Albarede, F. (1990). A major 2,1 Ga event of mafic magmatism in West Africa: an early stage of crustal accretion. *J. Geophys. Res., 95*, 17605-17629. https://doi.org/10.1029/JB095iB11p17605

Adingra, M. P. K., Coulibaly, Y., Ouattara, Z., & Coulibaly, I. (2018). Caractéristiques pétrographiques et géochimiques des métasédiments de la partie sud-est du bassin de la comoé (nord d'alépé- sud est de la côte d'ivoire). *Rev. RAMRES, 06*(02).

Arnould, A. (1961). Etude géologique des migmatites et des granites précambriens du nord-est de la Côte d'Ivoire et de la Haute-Volta méridionale. *Mémo BRGM., 3*, 175.

Beziat, D., Bourges, F., Debat, P., Lompo, M., Martin, F., & Tollon, F. (2000). A Paleo-proterozoic ultramafic-mafic assemblage and associated volcanic rocks of the Boromo greenstone belt: fractionates originating from island-arc volcanic activity in the West African craton. *Precambrian Research, 101*(1), 25-47. https://doi.org/10.1016/S0301-9268(99)00085-6

Boher, M. (1991). *Croissance crustale en Afrique de l'Ouest à 2,1 Ga. Apport de la Géochimie isotopique.* Doctorat, Univ. Nancy-I. pp. 180.

Boher, M., Abouchamy, W., Michard, A., Albarède, F., & Arndt, N. T. (1992). Crustal growth in West Africa at 2.1 Ga. *J. Geophys. Res., 97*, 345-369. https://doi.org/10.1029/91JB01640

Bonhomme, M. (1962). Contribution à l'étude géochronologique de la plate-forme de l'Ouest Africain. *Doctorat, Ann. Fac. Sc. Univ., Clermont-Ferrand, 5*, 62.

Coulibaly. (2018). *Petrologie des volcanites et des plutonites du sud du sillon birimien de toumodi-fetekro (Cote d'Ivoire): implications petrogénétique et tectonique*. Thèse de doctorat, Univ. Félix HOUPHOUËT –BOIGNY. pp. 252.

Cox, K. G., Bell, J. D., & Pankhurst, R. J. (1979). *The interpretation of igneous rocks.* George, Allen and Unwin, London. https://doi.org/10.1007/978-94-017-3373-1

Dampare, S. B., Shibata, T., Asiedu, D. K., Osae, S., & Banoeng-Yakubo B. (2008). Geochemistry of Paleoproterozoïc metavolcanic rocks from the southern Ashanti volcanic belt, Ghana: Petrogenetic and tectonic setting implications. *Precambrian Research, 162*, 403-423. https://doi.org/10.1016/j.precamres.2007.10.001

Daouda, Y. B. (1998). Lithostratigraphie et pétrologie des formations birimiennes de Toumodi-Fettêkro, Côte d'Ivoire : implication pour l'évolution crustale du Paléo-protérozoïque du craton Ouest-Africain. *Doctorat, Univ. Orléans-Géosciences, Mémoire, 737*, 191.

Debat, P., Nikiema, S., Mercier, A., Lompo, M., Beziat, D., Bourges, F., Roddaz, M., Salvi, S., Tollon, F., & Wenmenga, U. (2003). A new metamorphic constraint for the Eburnean orogeny from Paleoproterozoic formations of the Man shield (Aribinda and Tampelga countries, Burkina Faso). *Precambrian Research, 123*(1), 47-65. https://doi.org/10.1016/S0301-9268(03)00046-9

Doumbia, S. (1997). Géochimie, géochronologie et géologie structurale des formations birimiennes de la région de Katiola-Marabadiassa (centre nord de la Côte d'Ivoire). Evolution magmatique et contexte géodynamique du Paléoprotérozoïque. *Doctorat, Univ. Orléans, Mémoire BRGM, 276*, 253.

Fabre, R., Ledru, P., & Feybesse, J. L. (1993). *New geodynamic model for the Birimian calc-alkali magmatism from West-Africa: example of the Dianfla trough, Ivory Coast*. Early Proterozoic Symposium, Dakar-Sénégal. pp. 85-89.

Fabre, R., Ledru, P., & Milesi, J. P. (1990). Le protérozoïque inférieur (Birimien) du centre de la Côte d'Ivoire : évolution tectonique et corrélations. *Comptes rendus Académie des Sciences (Paris), 311*(II), 971-976.

Fabre, R., & Morel, B. (1993). Stratigraphie des unités birimiennes dans le centre de la Côte d'Ivoire (Afrique de l'Ouest). *Bulletin Société Géologique, France, 164*(4), 609-621.

Feybesse, J. L., Billa, M., Guerrot, C., Duguey, E., Lescuyer, J. L., Milesi, J. P., & Bouchot, V. (2006). The Paleoproterozoïc Ghanaian province: Geodynamic model and ore controls, including regional stress modeling. *Precambrian Research, 149*(3-4), 149-196. https://doi.org/10.1016/j.precamres.2006.06.003

Feybesse, J. L., & Milesi, J. P. (1994). The Archaean/Proterozoic contact zone in West Africa: a mountain belt of décollement thrusting and folding on a continental margin related to 2,1 Ga convergence of Archaean cratons? *Precambrian Research, 69*, 199-227. https://doi.org/10.1016/0301-9268(94)90087-6

Gnanzou, A. (2014). *Etude des séries volcanosédimentaires de la région de Dabakala (Nord-Est de la Côte d'Ivoire): Genèse et évolution magmatique. Contribution à la connaissance de la minéralisation aurifère de Bobosso dans la série de la Haute-Comoé*. Thèse unique, Univ. Paris-Sud XI, Faculté des Sciences d'Orsay, Mémoire. pp. 258.

Gueye, M., Ngom, P. M., Diène, M., Thiam, Y., Siegesmund, S., Wemmer, K., & Pawlig, S. (2008). Intrusive rocks and tectono-metamorphic evolution of the Mako Paleoproterozoic belt (Eastern Senegal, West Africa). *Journal of African Earth Sciences, 50*, 88-110. https://doi.org/10.1016/j.jafrearsci.2007.09.013

Herron, M. M. (1988). Geochemical classification of terrigenous sands and shales from core or log data. *J. Sed. Petrol., 58*, 820-829. https://doi.org/10.1306/212F8E77-2B24-11D7-8648000102C1865D

Hirdes, D., Davis, D. W., Lüdtke, G., & Konan, G. (1996). Two generations of Birimian (Paleoproterozoïc) volcanic belts in northeastern Côte d'Ivoire (West Africa): consequences for the Birimian controversy. *Precambrian Research, 80*, 173-191. https://doi.org/10.1016/S0301-9268(96)00011-3

Houssou, N. N., Coulibaly, Y., & Tourigny, G. (2011). Etude litho-structurale du gisement aurifère d'Agbaou, Côte d'Ivoire. *Journal Africain de Communication Scientifique et Technologique, 11*(January 2011), 1393-1407.

Houssou, N. N. (2013). *Etude pétrologique, structurale et métallogénique du gisement aurifère d'Agbaou, Divo, Côte d'Ivoire*. Thèse unique, Univ. Félix Houphouet Boigny-UFR STRM, Mémoire. pp. 257.

Irvine, T. N., & Baragar, W. R. A. (1971). A guide to the chemical classification of the common volcanic rocks. *Can. J. Earth Sci., 8*, 523-548. https://doi.org/10.1139/e71-055

Isnard, P. (1954). *Rapport d'ensemble sur le levé du contact Birimien-Granite à l'Ouest et au Sud d'Hiré et sur la prospection du champ filonien*. BUMIFOM, PCI Hiré. pp. 9.

Koffi, Y. A., Kouamelan, A. N., Kouadio, F. J-L. H., Teha, K. R., Kouassi, B. R., & Koffi, G. R. S. (2018). Pétrographie et origine des métasédiments du domaine SASCA (SW de la Côte d'Ivoire). *International Journal of Innovation and Applied Studies, 23,* 451-464.

Leake, M. H. (1992). *The petrogenesis and structural evolution of the Early Proterozoïc Fettèkro greenstone belt, Dabakala region, NE Côte d'Ivoire*. PhD. Thesis, University of Portsmouth, U.K. pp. 315.

Lemoine, S. (1988). *Evolution géologique de la région de Dabakala (NE de la Côte d'Ivoire) au Protérozoïque inférieur.* Doctorat ès Sciences, Univ. Clermont-Ferrand. pp. 388.

Lesher, C. M., Goodwin, A. M., Campbell, I. H., & Gorton, M. P. (1986). Trace element geochemistry of ore-associated and barren, felsic metavolcanic rocks in the Superior Province. *Canada Journal of Earth Sciences, 23*, 222-237. https://doi.org/10.1139/e86-025

Lompo, M. (2009). Geodynamic evolution of the 2.25-2.0 Ga Paleoproterozoïc magmatic rocks in the Man-Leo Shield of the West African Craton. A model of subsidence of an oceanic plateau. Geological Society of London. *Paleoproterozoïc Supercontinents and Global Evolution, S.P., 323*(1), 231-254. https://doi.org/10.1144/SP323.11

Lompo, M. (2010). Structural evolution of Paleoproterozoïc belts (Eburnean event) in the Man-Leo Shield, West African Craton. Key structures for vertical to transcurrent tectonics. *Journal of African Earth Sciences, 58,* 19-36. https://doi.org/10.1016/j.jafrearsci.2010.01.005

Milesi, J. P. (1989). West Africa gold deposits in their lower Proterozoïc lithostructural setting. *Chronique Recherche Minière, 497*, 3-98.

Milesi, J. P., Ledru, P., Feybesse, J. L., Dommanget, A., & Marcoux, E. (1992). Early Proterozoïc ore deposits and tectonics of the Birimian orogenic belt, West Africa. *Precambrian Research, 58*(1-4), 305-344. https://doi.org/10.1016/0301-9268(92)90123-6

Mortimer, J. (1990). *Evolution of early Proterozoïc Toumodi volcanic group and associated rocks, Ivory Coast*. Ph.D. Thesis, Portsmouth Polytechnic, U.K. pp. 244.

Olson, S. F. (1989). *Carte géologique de la concession de Hiré.* BHP Minerals, Archives de la SODEMI.

Ouattara, G., Koffi, G. B., Yao, K. A., Agoh, O., & Yao, D. B. (2008). Pétrographie et évolution structurale du synclinal d'Anikro dans la région de Toumodi, Centre de la Côte d'Ivoire. *Bioterre, Rev. Inter. Sci. de la Vie et de la Terre, 9*, 48-60.

Ouattara, Z. (2015). *Caractères lithostratigraphiques, structural, géochimique et métallogénique du gisement d'or de Bonikro, sillon birimien de Fettèkro, Centre-Sud de la Côte d'Ivoire*. Thèse unique, Université Félix Houphouët-Boigny, Côte d'Ivoire. pp. 275.

Ouédraogo, M. F. (1989). Eléments de synthèse sur l'évolution géostructurale et la métallogénie de la ceinture Birimienne de Boromo, protérozoïque inférieur, Burkina Faso, Afrique de l'Ouest. *Doctorat, Univ. Orléans, France, 89*, 207.

Papon, A. (1973). Géologie et minéralisations du Sud-ouest de la Côte d'Ivoire. *Mémoire du BRGM, Paris, 80*, 284.

Pearce, J. A. (1983). Role of the sub-continental lithosphere in magma genesis at active continental margins. In C. J. Hawkeworth & M. J. Norry (Eds.), *Continental basalts and mantle xenoliths* (pp. 230-249). Shiva, Nantwich.

Pearce, J. A., Harris, N. B. W., & Tindle, A. G. (1984). Trace element discrimination diagrams for the tectonic interpretation of granitic rocks. *J. Petrol., 25*, 956-983. https://doi.org/10.1093/petrology/25.4.956

Pearce, J. A., & Cann, J. R. (1973). Tectonic setting of basic volcanic rocks determined using trace element analyses. *Earth Planet. Sci. Lett., 19*, 290-300. https://doi.org/10.1016/0012-821X(73)90129-5

Pettijohn, F. J., Potter, P. E., & Siever, R. (1972). *Sand and sandstones.* Springer-Verlag, New York.

Pothin, K. B. K. (1993). Un exemple de volcanisme du Protérozoïque inférieur en Côte d'Ivoire: zone de subduction ou zone de cisaillement ? *Journal of African Earth Sciences, 16*(4), 437-443. https://doi.org/10.1016/0899-5362(93)90102-V

Potter, P. E. (1978). Petrology and chemistry of modern big river sands. *J. Geol., 86*, 423-449. https://doi.org/10.1086/649711

Pouclet, A., Doumbia, S., Vidal, M., Delor, C., & Bodinier, J. L. (1995). *Les deux phases volcaniques du sillon birimien de Katiola, centre nord de la Côte d'Ivoire : un modèle de l'évolution géotectonique-magmatique du Paléoprotérozoïque de l'Afrique de l'Ouest*. Séance spécialisée de la Société Géologique de France. pp. 29.

Roser, B. P., & Korsch, R. J. (1986). Determination of tectonic setting of sandstone-mudstone suites using SiO2 content and K2O/Na2O ratio. *J. Geol., 94*, 635-650. https://doi.org/10.1086/629071

Sun, S. S., & McDonough, W. F. (1989). Chemical and isotopic systematics of oceanic basalts: implications for mantle composition and processes. *Geological Society Special Publication, 42*, 313-345. https://doi.org/10.1144/GSL.SP.1989.042.01.19

Sylla, M., & Ngom, P. M. (1997). Le gisement d'or de Sabodala (Sénégal Oriental): une minéralisation filonienne d'origine hydrothermale remobilisée par une tectonique cisaillante. *Journal of African Earth Sciences, 25*(2), 183-192. https://doi.org/10.1016/S0899-5362(97)00097-3

Tagini, B. (1971). Esquisse structurale de la Côte d'Ivoire ; essai de géotectonique régionale. *Doctorat, Univ. Lausanne, Côte d'Ivoire (SODEMI), Bull., 5*, 302.

Taylor, P. N., Moorbath, S., Leube, A., & Hirdes, W. (1992). Early Proterozoïc crustal evolution in the Birimian of Ghana: constraints from geochronology isotope geochemistry. *Precambrian Research, 56*, 97-111. https://doi.org/10.1016/0301-9268(92)90086-4

Taylor, S. R., & McLennan, S. M. (1985). *The continental crust: its composition and evolution*. Blackwell Scientific Publication, Carlton. pp. 312.

Thompson, R. N. (1984). Dispatches from the basalt front. *1. Experiments. Proc. Geol. Ass., 95*, 249-262. https://doi.org/10.1016/S0016-7878(84)80011-5

Turner, P. (1995). *Evolution of the early Proterozoïc Boundiali-Bagoé Supracrustal Belt and associated granitic rocks, northern Côte d'Ivoire, West Africa*. Unpublished Ph.D. Thesis, University of Portsmouth. pp. 265.

Vidal, M., & Alric, G. (1994). The Paleoproterozoïc (Birimian) of Haute-Comoé in the West African craton, Ivory Coast: a transtensional back-arc basin. *Prec. Research, 65*, 207-229. https://doi.org/10.1016/0301-9268(94)90106-6

Vidal, M., Delor, C., Pouclet, A., Simeon, Y., & Alric, G. (1996). Evolution géodynamique de l'Afrique de l'Ouest entre 2,2 et 2 Ga : le style archéen des ceintures vertes et des ensembles sédimentaires birimiens du nord-est de la Côte d'Ivoire. *Bulletin de la Société Géologique de France, 167*, 307-319.

Vidal, M., Trap, P., & Faure, M. (2006). *Diversité des modèles d'évolution géodynamique au paléo-protérozoïque. Comparaison entre le craton ouest africain et le craton de chine du nord*. Manuscrit auteur, publié dans. 21ème Colloque de Géologie Africaine, Maputo: Mozambique.

Wilson, M. (1989). *Igneous Petrogenesis: a Global Tectonic Approach*. London (Unwin Hyman). pp. xx-466. https://doi.org/10.1007/978-1-4020-6788-4

Wood, D. A. (1980). The application of a Th-Hf-Ta diagram to problems of tectono-magmatic classification and to establishing the nature of crustal contamination of basaltic lavas of the British Tertiary volcanic province. *Earth Planet. Sci. Lett., 50*, 11-30. https://doi.org/10.1016/0012-821X(80)90116-8

Yacé, I. (1993). *Les complexes volcano-sédimentaires précambriens en Afrique de l'Ouest.* Symposium sur le protérozoïque inférieur, CIFEG.

Yacé, I. (1982). *Etude géologique du volcanisme Eburnéen dans les parties centrale et méridionale de la chaine précambrienne de Fettèkro*. Ministère des mines, République de la Côte d'Ivoire. pp. 156.

Yao, A. K. (1993). Le volcanisme du sillon de Boundiali, phénomène principal du Paléo-protérozoïque inférieur de cette région NNW de la Côte d'Ivoire. Pétrologie, géochimie, géochronologie. *Doctorat, Univ. Clermont-Ferrand, 2*, 218.

## Annexes

Annexe 1. Oxide chemical analysis and normative composition of basalts and basaltic andesites

| AGBAOU DEPOSIT | Basalts and basaltic andesites | | | | | | | |
|---|---|---|---|---|---|---|---|---|
| Samples | ADD250-154 | ADD355-203 | ADD232-135 | ARC217D-150 | ARC137D-178 | ADD219-147 | ADD225-135 | ADD329-149 |
| RAW VALUES | | | | | | | | |
| SiO2 | 37,677 | 40,269 | 39,771 | 38,69 | 39,63 | 53,513 | 46,927 | 45,399 |
| Al2O3 | 9,854 | 13,869 | 14,14 | 10,93 | 13,586 | 13,527 | 13,514 | 12,581 |
| Fe2O3 t | 12,309 | 10,062 | 9,002 | 11,126 | 12,709 | 10,224 | 8,875 | 11,965 |
| MnO | 0,177 | 0,136 | 0,159 | 0,141 | 0,178 | 0,167 | 0,136 | 0,185 |
| MgO | 6,48 | 7,516 | 4,651 | 6,416 | 8,265 | 5,493 | 5,899 | 5,349 |
| CaO | 11,84 | 8,023 | 10,575 | 12,383 | 9,449 | 11,361 | 10,505 | 10,087 |
| Na2O | 3,479 | 4,935 | 4,371 | 1,761 | 2,51 | 1,027 | 1,504 | 2,417 |
| K2O | 0,166 | 0,088 | 1,2 | 0,374 | 1,163 | <L.D. | 0,243 | <L.D. |
| TiO2 | 0,667 | 0,683 | 0,64 | 0,836 | 0,851 | 0,598 | 0,617 | 0,999 |
| P2O5 | 0,091 | 0,065 | 0,07 | 0,087 | 0,085 | 0,064 | 0,067 | 0,103 |
| PF | 16,305 | 13,098 | 12,93 | 17,265 | 10,663 | 2,957 | 10,512 | 10,296 |
| TOTAL | 99,05 | 98,74 | 97,51 | 100,01 | 99,09 | 98,93 | 98,80 | 99,38 |
| ANHYDROUS VALUES NORMALIZED TO 100 | | | | | | | | |
| SiO2 | 46,03 | 47,39 | 47,36 | 47,23 | 45,28 | 56,18 | 53,54 | 51,45 |
| TiO2 | 0,81 | 0,80 | 0,76 | 1,02 | 0,97 | 0,63 | 0,70 | 1,13 |
| Al2O3 | 12,04 | 16,32 | 16,84 | 13,34 | 15,52 | 14,20 | 15,42 | 14,26 |
| Fe2O3 calculated | 4,31 | 3,86 | 3,60 | 3,51 | 4,28 | 3,17 | 2,87 | 3,95 |
| FeO calculated | 9,66 | 7,18 | 6,41 | 9,06 | 9,21 | 6,81 | 6,53 | 8,64 |
| MnO | 0,22 | 0,16 | 0,19 | 0,17 | 0,20 | 0,18 | 0,16 | 0,21 |
| MgO | 7,92 | 8,85 | 5,54 | 7,83 | 9,44 | 5,77 | 6,73 | 6,06 |
| CaO | 14,46 | 9,44 | 12,59 | 15,12 | 10,80 | 11,93 | 11,99 | 11,43 |
| Na2O | 4,25 | 5,81 | 5,20 | 2,15 | 2,87 | 1,08 | 1,72 | 2,74 |
| K2O | 0,20 | 0,10 | 1,43 | 0,46 | 1,33 | 0,00 | 0,28 | 0,00 |
| P2O5 | 0,11 | 0,08 | 0,08 | 0,11 | 0,10 | 0,07 | 0,08 | 0,12 |
| TOTAL | 100,00 | 100,00 | 100,00 | 100,00 | 100,00 | 100,00 | 100,00 | 100,00 |
| Na2O + K2O | 4,45 | 5,91 | 6,63 | 2,61 | 4,20 | 1,08 | 1,99 | 2,74 |
| Fe2O3/FeO | 0,45 | 0,54 | 0,56 | 0,39 | 0,46 | 0,46 | 0,44 | 0,46 |
| CIPW STANDARD CALCULATION | | | | | | | | |
| Quartz | - | - | - | - | - | 17,15 | 8,5 | 3,62 |
| Corindon | - | - | - | - | - | - | - | - |
| Orthose | 1,18 | 0,59 | 8,44 | 2,72 | 7,85 | - | 1,65 | - |
| Albite | 8,07 | 22,17 | 8,41 | 12,79 | 10,78 | 9,13 | 14,54 | 23,16 |
| Anorthite | 13,18 | 18,16 | 18,38 | 25,38 | 25,53 | 33,87 | 33,51 | 26,6 |
| Néphéline | 15,1 | 14,6 | 19,27 | 2,92 | 7,3 | - | - | - |
| Diopside | 47,28 | 22,69 | 35,44 | 39,91 | 22,22 | 20,26 | 20,64 | 24,03 |
| Hypersthene | - | - | - | - | - | 13,64 | 15,48 | 14,42 |
| Olivine | 7,22 | 14,53 | 3,26 | 9,06 | 18,08 | - | - | - |
| Magnétite | 6,26 | 5,61 | 5,23 | 5,1 | 6,22 | 4,6 | 4,17 | 5,74 |
| Ilménite | 1,54 | 1,52 | 1,45 | 1,94 | 1,85 | 1,2 | 1,33 | 2,15 |
| Apatite | 0,24 | 0,17 | 0,17 | 0,24 | 0,22 | 0,15 | 0,17 | 0,26 |
| TOTAL | 100,07 | 100,04 | 100,05 | 100,06 | 100,05 | 100 | 99,99 | 99,98 |
| FELSIC MINERALS | | | | | | | | |
| Quartz | - | - | - | - | - | 29 | 15 | 7 |
| Feldspaths A. | 31 | 22 | 38 | 12 | 26 | 0 | 3 | 0 |
| Plagioclases | 40 | 58 | 36 | 82 | 62 | 71 | 83 | 93 |
| Foïdes | 29 | 21 | 26 | 6 | 12 | - | - | - |
| TOTAL | 100 | 101 | 100 | 100 | 100 | 100 | 101 | 100 |
| DIAGRAMS | | | | | | | | |
| Na2O+K2O | 4,45 | 5,91 | 6,63 | 2,61 | 4,20 | 1,08 | 1,99 | 2,74 |
| CaO+Na2O+K2O | 18,92 | 15,35 | 19,23 | 17,72 | 14,99 | 13,01 | 13,98 | 14,17 |
| Al2O3/(Na2O+K2O) | 2,70 | 2,76 | 2,54 | 5,12 | 3,70 | 13,17 | 7,74 | 5,21 |
| Al2O3/(CaO+Na2O+K2O) | 0,64 | 1,06 | 0,88 | 0,75 | 1,04 | 1,09 | 1,10 | 1,01 |
| Na2O/K2O | 20,96 | 56,08 | 3,64 | 4,71 | 2,16 | - | 6,19 | - |

Annexe 2. Chemical oxide analyses and normative composition of basalts and basaltic andesites

| AGBAOU DEPOSIT | Basalts and basaltic andesites | | | | | | | |
|---|---|---|---|---|---|---|---|---|
| Samples | ADD298-190 | ADD256-117 | ARC049D-164 | ARC217D-178 | ADD224-201 | ARC175D-139 | ARC116D-139 | ADD224-172 |
| RAW VALUES | | | | | | | | |
| SiO2 | 50,778 | 43,131 | 50,553 | 49,483 | 49,327 | 49,43 | 49,312 | 47,736 |
| Al2O3 | 13,498 | 10,558 | 14,115 | 13,259 | 14,934 | 14,481 | 14,886 | 12,674 |
| Fe2O3 t | 12,748 | 10,79 | 11,285 | 12,31 | 10,37 | 13,228 | 10,393 | 13,277 |
| MnO | 0,183 | 0,21 | 0,173 | 0,199 | 0,157 | 0,175 | 0,172 | 0,173 |
| MgO | 8,432 | 5,039 | 7,327 | 5,549 | 8,072 | 7,262 | 9,099 | 4,85 |
| CaO | 7,577 | 14,938 | 11,599 | 11,78 | 12,501 | 9,301 | 10,229 | 7,463 |
| Na2O | 2,422 | 1,742 | 1,442 | 1,339 | 1,729 | 1,572 | 2,382 | 3,453 |
| K2O | <L.D. | 0,232 | <L.D. | <L.D. | <L.D. | 0,056 | <L.D. | 0,149 |
| TiO2 | 0,835 | 0,845 | 0,841 | 1,021 | 0,689 | 1,079 | 0,682 | 1,547 |
| P2O5 | 0,085 | 0,081 | 0,084 | 0,101 | 0,07 | 0,11 | 0,071 | 0,165 |
| PF | 3,551 | 11,196 | 2,281 | 4,771 | 2,248 | 2,831 | 2,835 | 8,286 |
| TOTAL | 100,11 | 98,76 | 99,70 | 99,81 | 100,10 | 99,53 | 100,06 | 99,77 |
| ANHYDROUS VALUES NORMALIZED TO 100 | | | | | | | | |
| SiO2 | 53,07 | 49,70 | 52,32 | 52,55 | 50,79 | 51,62 | 51,10 | 52,69 |
| TiO2 | 0,87 | 0,97 | 0,87 | 1,08 | 0,71 | 1,13 | 0,71 | 1,71 |
| Al2O3 | 14,11 | 12,17 | 14,61 | 14,08 | 15,38 | 15,12 | 15,43 | 13,99 |
| Fe2O3 calculated | 4,18 | 3,40 | 3,41 | 3,73 | 3,13 | 4,02 | 3,30 | 4,78 |
| FeO calculated | 8,23 | 8,13 | 7,44 | 8,41 | 6,79 | 8,81 | 6,72 | 8,89 |
| MnO | 0,19 | 0,24 | 0,18 | 0,21 | 0,16 | 0,18 | 0,18 | 0,19 |
| MgO | 8,81 | 5,81 | 7,58 | 5,89 | 8,31 | 7,58 | 9,43 | 5,35 |
| CaO | 7,92 | 17,21 | 12,00 | 12,51 | 12,87 | 9,71 | 10,60 | 8,24 |
| Na2O | 2,53 | 2,01 | 1,49 | 1,42 | 1,78 | 1,64 | 2,47 | 3,81 |
| K2O | 0,00 | 0,27 | 0,00 | 0,00 | 0,00 | 0,06 | 0,00 | 0,16 |
| P2O5 | 0,09 | 0,09 | 0,09 | 0,11 | 0,07 | 0,11 | 0,07 | 0,18 |
| TOTAL | 100,00 | 100,00 | 100,00 | 100,00 | 100,00 | 100,00 | 100,00 | 100,00 |
| Na2O + K2O | 2,53 | 2,27 | 1,49 | 1,42 | 1,78 | 1,70 | 2,47 | 3,98 |
| Fe2O3/FeO | 0,51 | 0,42 | 0,46 | 0,44 | 0,46 | 0,46 | 0,49 | 0,54 |
| CIPW STANDARD CALCULATION | | | | | | | | |
| Quartz | 6,22 | 4,44 | - | 8,06 | 10,38 | 2,95 | 7,97 | 0,76 |
| Corindon | - | - | - | - | - | - | - | - |
| Orthose | - | 0,94 | 1,59 | - | - | - | 0,35 | - |
| Albite | 21,39 | 32,21 | 16,99 | 12,59 | 12 | 15,05 | 13,86 | 20,88 |
| Anorthite | 27,13 | 20,59 | 23,38 | 33,16 | 32,03 | 33,96 | 33,37 | 31 |
| Néphéline | - | - | - | - | - | - | - | - |
| Diopside | 9,36 | 15,67 | 50,39 | 20,9 | 24,04 | 23,75 | 11,46 | 16,98 |
| Hypersthène | 27,92 | 15,52 | 0,68 | 18,45 | 13,83 | 18,21 | 24,57 | 24,04 |
| Olivine | - | - | 0,03 | - | - | - | - | - |
| Magnétite | 6,07 | 6,94 | 4,94 | 4,95 | 5,42 | 4,55 | 5,84 | 4,79 |
| Ilménite | 1,66 | 3,25 | 1,85 | 1,66 | 2,05 | 1,35 | 2,15 | 1,35 |
| Apatite | 0,2 | 0,39 | 0,2 | 0,2 | 0,24 | 0,15 | 0,24 | 0,15 |
| TOTAL | 99,95 | 99,95 | 100,05 | 99,97 | 99,99 | 99,97 | 99,81 | 99,95 |
| FELSIC MINERALS | | | | | | | | |
| Quartz | 11 | 8 | 0 | 15 | 19 | 6 | 14 | 1 |
| Feldspaths A. | 0 | 2 | 4 | 0 | 0 | 0 | 1 | 0 |
| Plagioclases | 89 | 91 | 96 | 85 | 81 | 94 | 85 | 99 |
| Foïdes | - | - | - | - | - | - | - | - |
| TOTAL | 100 | 101 | 100 | 100 | 100 | 100 | 100 | 100 |
| DIAGRAMS | | | | | | | | |
| Na2O+K2O | 2,53 | 2,27 | 1,49 | 1,42 | 1,78 | 1,70 | 2,47 | 3,98 |
| CaO+Na2O+K2O | 10,45 | 19,49 | 13,50 | 13,93 | 14,65 | 11,41 | 13,07 | 12,21 |
| Al2O3/(Na2O+K2O) | 5,57 | 5,35 | 9,79 | 9,90 | 8,64 | 8,89 | 6,25 | 3,52 |
| Al2O3/(CaO+Na2O+K2O) | 1,35 | 0,62 | 1,08 | 1,01 | 1,05 | 1,33 | 1,18 | 1,15 |
| Na2O/K2O | - | 7.51 | - | - | - | 28.07 | - | 23.17 |

Annexe 3. Chemical oxide analysis and normative composition of pyroclastites and andesites

| AGBAOU DEPOSIT | Pyroclastics | | | | Andesites | |
|---|---|---|---|---|---|---|
| Samples | ADD222-227 | ADD224-315 | ADD355-255 | ADD232-169 | ARC124D-166 | ARC142D-231 |
| RAW VALUES | | | | | | |
| SiO2 | 49,195 | 46,748 | 46,771 | 61,502 | 50,331 | 50,221 |
| Al2O3 | 12,482 | 12,183 | 12,139 | 13,14 | 15,913 | 16,164 |
| Fe2O3 t | 10,992 | 8,263 | 7,358 | 5,948 | 8,32 | 9,785 |
| MnO | 0,183 | 0,151 | 0,135 | 0,082 | 0,13 | 0,15 |
| MgO | 8,951 | 7,074 | 6,625 | 4,21 | 3,883 | 5,211 |
| CaO | 8,991 | 9,536 | 8,178 | 4,626 | 7,828 | 7,829 |
| Na2O | 1,622 | 1,897 | 2,694 | 4,525 | 5,254 | 2,956 |
| K2O | 2,256 | 1,145 | 1,642 | 0,094 | 0,416 | 1,435 |
| TiO2 | 0,847 | 0,786 | 0,542 | 0,495 | 0,864 | 0,94 |
| P2O5 | 0,378 | 0,309 | 0,196 | 0,13 | 0,435 | 0,42 |
| PF | 2,908 | 10,758 | 13,231 | 4,101 | 6,018 | 5,009 |
| TOTAL | 98,81 | 98,85 | 99,51 | 98,85 | 99,39 | 100,12 |
| ANHYDROUS VALUES NORMALIZED TO 100 | | | | | | |
| SiO2 | 51,69 | 53,41 | 54,52 | 65,15 | 54,20 | 53,16 |
| TiO2 | 0,89 | 0,90 | 0,63 | 0,52 | 0,93 | 0,99 |
| Al2O3 | 13,12 | 13,92 | 14,15 | 13,92 | 17,14 | 17,11 |
| Fe2O3 calculated | 3,90 | 2,93 | 2,90 | 2,55 | 3,41 | 3,66 |
| FeO calculated | 6,88 | 5,86 | 5,11 | 3,38 | 4,99 | 6,03 |
| MnO | 0,19 | 0,17 | 0,16 | 0,09 | 0,14 | 0,16 |
| MgO | 9,41 | 8,08 | 7,72 | 4,46 | 4,18 | 5,52 |
| CaO | 9,45 | 10,90 | 9,53 | 4,90 | 8,43 | 8,29 |
| Na2O | 1,70 | 2,17 | 3,14 | 4,79 | 5,66 | 3,13 |
| K2O | 2,37 | 1,31 | 1,91 | 0,10 | 0,45 | 1,52 |
| P2O5 | 0,40 | 0,35 | 0,23 | 0,14 | 0,47 | 0,44 |
| TOTAL | 100,00 | 100,00 | 100,00 | 100,00 | 100,00 | 100,00 |
| Na2O + K2O | 4,07 | 3,48 | 5,05 | 4,89 | 6,11 | 4,65 |
| Fe2O3/FeO | 0,57 | 0,50 | 0,57 | 0,75 | 0,68 | 0,61 |
| CIPW STANDARD CALCULATION | | | | | | |
| Quartz | 4,05 | 0,82 | 0,66 | 20,2 | - | 3,54 |
| Corindon | - | - | - | - | - | - |
| Orthose | 7,73 | 13,99 | 11,27 | 0,59 | 2,66 | 8,97 |
| Albite | 18,34 | 14,37 | 26,54 | 40,49 | 47,84 | 26,46 |
| Anorthite | 24,36 | 21,16 | 18,87 | 16,18 | 20,03 | 28,13 |
| Néphéline | - | - | - | - | - | - |
| Diopside | 22,05 | 18,58 | 21,58 | 5,77 | 15,18 | 8,2 |
| Hypersthène | 16,68 | 22,77 | 15,11 | 11,73 | 2,15 | 16,45 |
| Olivine | - | - | - | - | 4,34 | - |
| Magnétite | 4,26 | 5,67 | 4,21 | 3,7 | 4,95 | 5,32 |
| Ilménite | 1,71 | 1,69 | 1,2 | 0,99 | 1,77 | 1,88 |
| Apatite | 0,76 | 0,87 | 0,5 | 0,31 | 1,03 | 0,96 |
| TOTAL | 99,94 | 99,92 | 99,94 | 99,96 | 99,95 | 99,91 |
| FELSIC MINERALS | | | | | | |
| Quartz | 7 | 2 | 1 | 26 | 0 | 5 |
| Feldspaths A. | 14 | 28 | 20 | 1 | 4 | 13 |
| Plagioclases | 78 | 71 | 79 | 73 | 96 | 81 |
| Foïdes | - | - | - | - | - | - |
| TOTAL | 99 | 101 | 100 | 100 | 100 | 99 |
| DIAGRAMS | | | | | | |
| Na2O+K2O | 4,07 | 3,48 | 5,05 | 4,89 | 6,11 | 4,65 |
| CaO+Na2O+K2O | 13,52 | 14,37 | 14,59 | 9,79 | 14,54 | 12,93 |
| Al2O3/(Na2O+K2O) | 3,22 | 4,00 | 2,80 | 2,84 | 2,81 | 3,68 |
| Al2O3/(CaO+Na2O+K2O) | 0,97 | 0,97 | 0,97 | 1,42 | 1,18 | 1,32 |
| Na2O/K2O | 0,72 | 1,66 | 1,64 | 48,14 | 12,63 | 2,06 |

Annexe 4. Chemical oxide analysis and normative composition of acid lavas, plutonites and sediments

| AGBAOU DEPOSIT | Rhyodacites | Rhyolites | | Gabbros | | Diorites | Metasediments | |
|---|---|---|---|---|---|---|---|---|
| Samples | ARC049D-181 | ARC169D-157 | ARC172D-153 | ADD232-154 | ARC215D-201 | ADD272-252 | ADD355-261 | ARC208D-228 |
| RAW VALUES | | | | | | | | |
| $SiO_2$ | 69,93 | 75,116 | 72,422 | 46,992 | 44,231 | 47,07 | 52,768 | 61,32 |
| $Al_2O_3$ | 14,767 | 14,585 | 15,297 | 14,776 | 11,323 | 11,717 | 14,333 | 14,231 |
| $Fe_2O_3$ t | 1,908 | 0,768 | 1,159 | 9,816 | 8,006 | 6,369 | 7,783 | 5,336 |
| MnO | 0,02 | 0,024 | 0,016 | 0,147 | 0,127 | 0,111 | 0,241 | 0,077 |
| MgO | 0,711 | 0,101 | 0,444 | 5,568 | 10,066 | 7,804 | 2,057 | 1,715 |
| CaO | 2,371 | 1,289 | 1,74 | 8,209 | 8,229 | 7,745 | 5,873 | 5,523 |
| $Na_2O$ | 4,757 | 5,345 | 7,018 | 3,393 | 2,818 | 4,235 | 6,056 | 0,791 |
| $K_2O$ | 2,23 | 1,635 | 0,589 | 2,154 | 0,882 | 0,669 | 1,021 | 3,325 |
| $TiO_2$ | 0,28 | 0,047 | 0,14 | 0,867 | 0,687 | 0,578 | 0,806 | 0,564 |
| $P_2O_5$ | 0,073 | <L.D. | 0,04 | 0,353 | 0,248 | 0,299 | 0,233 | 0,159 |
| PF | 2,919 | 1,643 | 1,537 | 7,034 | 12,854 | 12,032 | 7,36 | 6,409 |
| TOTAL | 99,97 | 100,55 | 100,40 | 99,31 | 99,47 | 98,63 | 98,53 | 99,45 |
| ANHYDROUS VALUES NORMALIZED TO 100 | | | | | | | | |
| $SiO_2$ | 72,13 | 75,97 | 73,30 | 51,27 | 51,39 | 54,62 | 58,17 | 66,14 |
| $TiO_2$ | 0,29 | 0,05 | 0,14 | 0,95 | 0,80 | 0,67 | 0,89 | 0,61 |
| $Al_2O_3$ | 15,23 | 14,75 | 15,48 | 16,12 | 13,16 | 13,60 | 15,80 | 15,35 |
| $Fe_2O_3$ calculated | 0,97 | 0,40 | 0,60 | 3,91 | 2,92 | 2,60 | 3,62 | 2,26 |
| FeO calculated | 0,90 | 0,34 | 0,51 | 6,12 | 5,74 | 4,31 | 4,47 | 3,15 |
| MnO | 0,02 | 0,02 | 0,02 | 0,16 | 0,15 | 0,13 | 0,27 | 0,08 |
| MgO | 0,73 | 0,10 | 0,45 | 6,08 | 11,70 | 9,06 | 2,27 | 1,85 |
| CaO | 2,45 | 1,30 | 1,76 | 8,96 | 9,56 | 8,99 | 6,47 | 5,96 |
| $Na_2O$ | 4,91 | 5,41 | 7,10 | 3,70 | 3,27 | 4,91 | 6,68 | 0,85 |
| $K_2O$ | 2,30 | 1,65 | 0,60 | 2,35 | 1,02 | 0,78 | 1,13 | 3,59 |
| $P_2O_5$ | 0,08 | 0,00 | 0,04 | 0,39 | 0,29 | 0,35 | 0,26 | 0,17 |
| TOTAL | 100,00 | 100,00 | 100,00 | 100,00 | 100,00 | 100,00 | 100,00 | 100,00 |
| $Na_2O + K_2O$ | 7,21 | 7,06 | 7,70 | 6,05 | 4,30 | 5,69 | 7,80 | 4,44 |
| $Fe_2O_3/FeO$ | 1,07 | 1,17 | 1,18 | 0,64 | 0,51 | 0,60 | 0,81 | 0,72 |
| CIPW STANDARD CALCULATION | | | | | | | | |
| Quartz | 28,52 | 35,2 | 25,32 | - | - | - | | |
| Corindon | 0,4 | 1,71 | 0,05 | - | - | - | | |
| Orthose | 13,58 | 9,74 | 3,54 | 13,87 | 6,02 | 4,6 | | |
| Albite | 41,5 | 45,73 | 60,02 | 28,95 | 27,64 | 41,5 | | |
| Anorthite | 11,63 | 6,44 | 8,47 | 20,43 | 18,21 | 12,76 | | |
| Néphéline | - | - | - | 1.26 | - | - | | |
| Diopside | - | - | - | 17.36 | 21.79 | 23.52 | | |
| Hypersthène | 2,22 | 0,5 | 1,36 | - | 5.04 | 0.52 | | |
| Olivine | - | - | - | 9,78 | 14,91 | 11,29 | | |
| Magnétite | 1,41 | 0,58 | 0,87 | 5,68 | 4,24 | 3,78 | | |
| Ilménite | 0,55 | 0,1 | 0,27 | 1,81 | 1,52 | 1,27 | | |
| Apatite | 0,17 | | 0,09 | 0,85 | 0,63 | 0,76 | | |
| TOTAL | 99,98 | 100 | 99,99 | 99,99 | 100 | 100 | | |
| FELSIC MINERALS | | | | | | | | |
| Quartz | 30 | 36 | 26 | - | 0 | 0 | | |
| Feldspaths A. | 14 | 57 | 65 | 23 | 12 | 8 | | |
| Plagioclases | 56 | 7 | 9 | 75 | 88 | 92 | | |
| Foïdes | - | - | - | 2 | - | - | | |
| TOTAL | 100 | 100 | 100 | 100 | 100 | 100 | | |
| DIAGRAMS | | | | | | | | |
| $Na_2O+K_2O$ | 7,21 | 7,06 | 7,70 | 6,05 | 4,30 | 5,69 | 7,80 | 4,44 |
| $CaO+Na_2O+K_2O$ | 9,65 | 8,36 | 9,46 | 15,01 | 13,86 | 14,68 | 14,27 | 10,40 |
| $Al_2O_3/(Na_2O+K_2O)$ | 2,11 | 2,09 | 2,01 | 2,66 | 3,06 | 2,39 | 2,03 | 3,46 |
| $Al_2O_3/(CaO+Na_2O+K_2O)$ | 1,58 | 1,76 | 1,64 | 1,07 | 0,95 | 0,93 | 1,11 | 1,48 |
| $Na_2O/K_2O$ | 2,13 | 3,27 | 11,92 | 1,58 | 3,20 | 6,33 | 5,93 | 0,24 |

Annexe 5. Trace elements and rare earths in basalts and basaltic andesites

| AGBAOU DEPOSIT | Basalts and basaltic andesites | | | | | | | |
|---|---|---|---|---|---|---|---|---|
| Samples | ADD250-154 | ADD355-203 | ADD232-135 | ARC217D-150 | ARC137D-178 | ADD219-147 | ADD225-135 | ADD329-149 |
| TRACES | | | | | | | | |
| As | 80,88 | 164,20 | 15,21 | 61,60 | 62,39 | 16,77 | 48,96 | 2,71 |
| Ba | 10,61 | 18,97 | 103,70 | 19,32 | 89,36 | 4,65 | 25,90 | 11,56 |
| Be | <L.D. | <L.D. | <L.D. | <L.D. | <L.D. | <L.D. | <L.D. | <L.D. |
| Bi | 0,48 | <L.D. | 0,35 | <L.D. | <L.D. | <L.D. | <L.D. | <L.D. |
| Cd | <L.D. | <L.D. | <L.D. | <L.D. | <L.D. | <L.D. | <L.D. | <L.D. |
| Co | 39,09 | 46,25 | 41,81 | 44,22 | 45,69 | 43,14 | 42,40 | 46,47 |
| Cr | 167,70 | 374,80 | 365,30 | 164,50 | 203,60 | 366,80 | 341,30 | 158,90 |
| Cs | 0,54 | 0,28 | 1,11 | 0,82 | 3,60 | <L.D. | 0,35 | <L.D. |
| Cu | 112,30 | 96,29 | 140,50 | 96,59 | 115,50 | 140,90 | 77,01 | 72,17 |
| Ga | 12,66 | 13,98 | 14,06 | 12,32 | 14,71 | 13,24 | 12,43 | 14,92 |
| Ge | 0,81 | 1,01 | 1,00 | 1,89 | 1,15 | 1,56 | 1,55 | 1,33 |
| Hf | 0,99 | 1,00 | 0,97 | 1,19 | 1,24 | 0,92 | 0,94 | 1,66 |
| In | <L.D. | <L.D. | <L.D. | <L.D. | <L.D. | <L.D. | <L.D. | <L.D. |
| Mo | 1,95 | <L.D. | 0,55 | 0,64 | <L.D. | 0,50 | <L.D. | 0,36 |
| Nb | 1,25 | 1,28 | 1,28 | 1,57 | 1,65 | 1,21 | 1,18 | 2,16 |
| Ni | 103,20 | 173,70 | 177,80 | 106,60 | 114,00 | 177,00 | 151,10 | 90,12 |
| Pb | 2,41 | 2,12 | 8,36 | <L.D. | 1,95 | 1,06 | <L.D. | <L.D. |
| Rb | 7,47 | 2,21 | 41,90 | 12,49 | 40,02 | 0,44 | 6,81 | <L.D. |
| Sb | <L.D. | <L.D. | 0,62 | 0,67 | <L.D. | 0,92 | 0,70 | <L.D. |
| Sn | 0,70 | 0,58 | 0,77 | 0,67 | 0,83 | <L.D. | <L.D. | 0,73 |
| Sr | 111,60 | 129,50 | 150,20 | 78,89 | 75,87 | 63,66 | 133,90 | 93,21 |
| Ta | 0,19 | 0,15 | 0,17 | 0,16 | 0,21 | 0,71 | 0,12 | 0,29 |
| Th | 0,12 | 0,12 | 0,11 | 0,14 | 0,13 | 0,11 | 0,10 | 0,19 |
| U | 0,05 | 0,05 | 0,08 | 0,13 | 0,05 | <L.D. | 0,05 | 0,10 |
| V | 230,40 | 245,20 | 252,40 | 235,50 | 280,40 | 216,80 | 214,60 | 293,10 |
| W | 3,95 | 7,67 | 5,62 | 1,32 | 1,23 | <L.D. | 0,37 | <L.D. |
| Y | 15,93 | 15,23 | 13,32 | 16,88 | 17,05 | 13,68 | 13,56 | 22,26 |
| Zn | 70,08 | 93,62 | 68,48 | 74,14 | 107,70 | 67,95 | 70,49 | 92,79 |
| Zr | 35,39 | 35,57 | 34,21 | 43,97 | 44,94 | 31,80 | 32,38 | 59,55 |
| RARE EARTHS | | | | | | | | |
| La | 1,43 | 1,58 | 1,51 | 1,99 | 1,63 | 1,53 | 1,54 | 2,61 |
| Ce | 4,11 | 4,34 | 4,04 | 5,46 | 4,69 | 4,22 | 4,20 | 7,08 |
| Pr | 0,65 | 0,68 | 0,63 | 0,91 | 0,77 | 0,66 | 0,66 | 1,13 |
| Nd | 3,69 | 3,93 | 3,61 | 4,86 | 4,14 | 3,74 | 3,73 | 6,42 |
| Sm | 1,37 | 1,40 | 1,26 | 1,70 | 1,51 | 1,32 | 1,32 | 2,18 |
| Eu | 0,58 | 0,48 | 0,61 | 0,70 | 0,47 | 0,53 | 0,55 | 0,89 |
| Gd | 2,03 | 1,95 | 1,79 | 2,36 | 2,26 | 1,88 | 1,83 | 3,09 |
| Tb | 0,37 | 0,36 | 0,33 | 0,42 | 0,41 | 0,34 | 0,33 | 0,55 |
| Dy | 2,55 | 2,48 | 2,24 | 2,79 | 2,74 | 2,27 | 2,18 | 3,66 |
| Ho | 0,55 | 0,53 | 0,49 | 0,61 | 0,60 | 0,49 | 0,48 | 0,78 |
| Er | 1,65 | 1,59 | 1,42 | 1,76 | 1,76 | 1,42 | 1,43 | 2,31 |
| Tm | 0,25 | 0,25 | 0,22 | 0,27 | 0,28 | 0,22 | 0,22 | 0,36 |
| Yb | 1,71 | 1,71 | 1,51 | 1,82 | 1,94 | 1,50 | 1,53 | 2,42 |
| Lu | 0,27 | 0,27 | 0,24 | 0,28 | 0,31 | 0,24 | 0,24 | 0,37 |

Annexe 6. Trace elements and rare earths in basalts and basaltic andesites

| AGBAOU DEPOSIT | Basalts and basaltic andesites | | | | | | | |
|---|---|---|---|---|---|---|---|---|
| Samples | ADD298-190 | ADD256-117 | ARC049D-164 | ARC217D-178 | ADD224-201 | ARC175D-139 | ARC116D-139 | ADD224-172 |
| TRACES | | | | | | | | |
| As | 43,45 | <L.D. | 5,14 | 3,57 | 5,36 | 4,76 | 3,72 | <L.D. |
| Ba | 6,02 | 52,31 | 6,77 | 6,57 | 4,62 | 11,29 | 6,20 | 67,81 |
| Be | <L.D. | <L.D. | <L.D. | <L.D. | <L.D. | <L.D. | <L.D. | <L.D. |
| Bi | <L.D. | <L.D. | <L.D. | <L.D. | <L.D. | <L.D. | <L.D. | <L.D. |
| Cd | 0,17 | <L.D. | 0,16 | 0,18 | <L.D. | <L.D. | 0,18 | <L.D. |
| Co | 51,89 | 38,95 | 43,89 | 46,19 | 42,53 | 51,24 | 43,46 | 49,08 |
| Cr | 210,80 | 134,40 | 298,50 | 217,70 | 364,00 | 189,40 | 362,70 | 107,60 |
| Cs | <L.D. | 1,23 | <L.D. | <L.D. | <L.D. | <L.D. | <L.D. | 1,03 |
| Cu | 121,00 | 107,70 | 105,50 | 89,43 | 100,30 | 93,23 | 105,50 | 98,52 |
| Ga | 14,93 | 11,73 | 14,31 | 15,65 | 12,99 | 16,46 | 13,02 | 16,80 |
| Ge | 1,51 | 0,86 | 1,58 | 1,55 | 1,38 | 1,64 | 1,17 | 1,34 |
| Hf | 1,29 | 1,24 | 1,18 | 1,54 | 0,97 | 1,57 | 0,98 | 2,30 |
| In | <L.D. | <L.D. | <L.D. | <L.D. | <L.D. | <L.D. | <L.D. | <L.D. |
| Mo | <L.D. | 0,49 | 0,50 | 0,59 | 0,43 | 0,57 | 0,39 | 0,68 |
| Nb | 1,67 | 1,79 | 1,80 | 2,05 | 1,71 | 2,14 | 1,55 | 3,31 |
| Ni | 116,20 | 73,65 | 117,70 | 107,00 | 154,50 | 122,90 | 168,10 | 72,71 |
| Pb | 1,62 | <L.D. | <L.D. | <L.D. | <L.D. | <L.D. | <L.D. | <L.D. |
| Rb | 0,58 | 9,67 | 1,27 | 0,55 | 0,45 | 1,50 | 0,64 | 5,49 |
| Sb | 0,34 | <L.D. | 0,88 | 0,73 | 1,44 | 0,24 | 1,02 | <L.D. |
| Sn | 0,67 | <L.D. | 0,57 | 0,74 | <L.D. | 0,77 | <L.D. | 1,17 |
| Sr | 61,21 | 71,48 | 166,50 | 96,88 | 267,90 | 138,90 | 187,90 | 85,89 |
| Ta | 0,78 | 0,53 | 1,62 | 0,24 | 3,17 | 0,51 | 1,66 | 0,64 |
| Th | 0,15 | 0,18 | 0,16 | 0,19 | 0,11 | 0,20 | 0,13 | 0,29 |
| U | 0,06 | 0,15 | 0,05 | 0,07 | 0,05 | 0,07 | 0,05 | 0,10 |
| V | 273,40 | 226,80 | 261,00 | 296,90 | 225,10 | 294,60 | 225,90 | 374,40 |
| W | 0,63 | 0,31 | <L.D. | 0,68 | <L.D. | <L.D. | <L.D. | <L.D. |
| Y | 19,23 | 17,57 | 18,35 | 22,18 | 14,28 | 22,69 | 14,82 | 28,70 |
| Zn | 99,51 | 63,77 | 83,28 | 94,32 | 73,84 | 108,90 | 76,69 | 122,80 |
| Zr | 45,12 | 45,47 | 43,05 | 55,13 | 34,46 | 58,01 | 35,14 | 83,77 |
| RARE EARTHS | | | | | | | | |
| La | 2,21 | 2,21 | 2,07 | 2,55 | 1,61 | 2,74 | 1,59 | 3,98 |
| Ce | 5,93 | 5,91 | 5,60 | 7,02 | 4,40 | 7,46 | 4,51 | 10,76 |
| Pr | 0,93 | 0,94 | 0,90 | 1,12 | 0,70 | 1,18 | 0,74 | 1,74 |
| Nd | 5,35 | 4,96 | 4,96 | 6,31 | 3,90 | 6,47 | 4,00 | 9,09 |
| Sm | 1,86 | 1,71 | 1,75 | 2,18 | 1,36 | 2,24 | 1,40 | 3,04 |
| Eu | 0,74 | 0,49 | 0,73 | 0,88 | 0,58 | 0,85 | 0,57 | 1,09 |
| Gd | 2,52 | 2,34 | 2,43 | 3,05 | 1,93 | 3,06 | 1,97 | 3,96 |
| Tb | 0,46 | 0,42 | 0,43 | 0,55 | 0,34 | 0,55 | 0,36 | 0,71 |
| Dy | 3,15 | 2,84 | 2,93 | 3,66 | 2,35 | 3,69 | 2,42 | 4,78 |
| Ho | 0,68 | 0,61 | 0,63 | 0,79 | 0,50 | 0,79 | 0,52 | 1,01 |
| Er | 2,03 | 1,82 | 1,88 | 2,33 | 1,50 | 2,36 | 1,56 | 2,96 |
| Tm | 0,31 | 0,28 | 0,28 | 0,36 | 0,24 | 0,36 | 0,24 | 0,44 |
| Yb | 2,11 | 1,90 | 1,93 | 2,43 | 1,55 | 2,48 | 1,61 | 3,00 |
| Lu | 0,33 | 0,31 | 0,31 | 0,39 | 0,25 | 0,39 | 0,25 | 0,48 |

Annexe 7. Trace elements and rare earths in pyroclastites and andesites

| AGBAOU DEPOSIT | Pyroclastics | | | | Andesites | |
|---|---|---|---|---|---|---|
| Samples | ADD222-227 | ADD224-315 | ADD355-255 | ADD232-169 | ARC124D-166 | ARC142D-231 |
| TRACES | | | | | | |
| As | < L.D. | 23,41 | 78,54 | 1,60 | 12,84 | 9,13 |
| Ba | 700,70 | 233,00 | 364,10 | 50,33 | 255,80 | 631,70 |
| Be | 1,81 | < L.D. | < L.D. | < L.D. | 1,13 | 1,15 |
| Bi | < L.D. | < L.D. | < L.D. | < L.D. | 0,15 | 0,14 |
| Cd | < L.D. | < L.D. | < L.D. | < L.D. | < L.D. | < L.D. |
| Co | 38,25 | 31,08 | 30,74 | 24,23 | 27,15 | 34,55 |
| Cr | 513,10 | 517,70 | 328,90 | 372,30 | 35,86 | 64,94 |
| Cs | 3,42 | 2,92 | 1,04 | 0,26 | 4,16 | 9,66 |
| Cu | 106,40 | 49,60 | 49,17 | 15,28 | 52,62 | 60,08 |
| Ga | 13,58 | 15,53 | 16,53 | 18,11 | 17,04 | 18,26 |
| Ge | 1,60 | 1,35 | 1,06 | 1,05 | 1,22 | 1,17 |
| Hf | 1,46 | 2,60 | 2,45 | 2,83 | 3,65 | 3,59 |
| In | < L.D. | < L.D. | < L.D. | < L.D. | < L.D. | < L.D. |
| Mo | 0,41 | < L.D. | 0,55 | 1,00 | 0,58 | 0,83 |
| Nb | 2,82 | 4,06 | 2,63 | 4,36 | 6,48 | 6,08 |
| Ni | 96,56 | 72,27 | 137,10 | 137,70 | 41,49 | 71,61 |
| Pb | 6,95 | 5,36 | 3,62 | 4,75 | 7,26 | 8,13 |
| Rb | 74,04 | 39,45 | 45,63 | 2,59 | 25,26 | 52,90 |
| Sb | 0,60 | < L.D. | < L.D. | 0,35 | 0,68 | 0,31 |
| Sn | 1,04 | 1,62 | 0,97 | 1,09 | 1,37 | 1,38 |
| Sr | 364,10 | 340,30 | 292,60 | 511,60 | 569,30 | 702,90 |
| Ta | 0,21 | 0,46 | 0,21 | 0,47 | 0,64 | 0,54 |
| Th | 1,43 | 2,66 | 3,44 | 1,99 | 4,00 | 3,75 |
| U | 0,47 | 1,20 | 0,91 | 0,64 | 1,27 | 1,19 |
| V | 243,80 | 205,70 | 144,00 | 84,39 | 171,00 | 205,30 |
| W | 0,83 | 2,36 | 7,27 | 0,41 | 0,73 | 0,65 |
| Y | 17,86 | 19,18 | 11,90 | 10,97 | 21,73 | 23,10 |
| Zn | 90,73 | 76,09 | 58,67 | 75,13 | 81,57 | 97,24 |
| Zr | 53,27 | 97,83 | 94,48 | 108,90 | 154,70 | 147,00 |
| RARE EARTHS | | | | | | |
| La | 9,58 | 19,01 | 20,70 | 13,80 | 32,58 | 31,08 |
| Ce | 20,02 | 39,52 | 43,04 | 27,46 | 67,13 | 64,81 |
| Pr | 2,61 | 4,90 | 5,22 | 3,15 | 8,22 | 8,12 |
| Nd | 12,56 | 21,94 | 22,38 | 13,37 | 34,18 | 34,83 |
| Sm | 3,19 | 4,65 | 4,38 | 2,75 | 6,56 | 6,80 |
| Eu | 1,04 | 1,37 | 1,28 | 0,83 | 1,86 | 1,91 |
| Gd | 3,42 | 4,11 | 3,21 | 2,41 | 5,18 | 5,45 |
| Tb | 0,52 | 0,62 | 0,42 | 0,36 | 0,71 | 0,76 |
| Dy | 3,16 | 3,52 | 2,23 | 2,00 | 3,87 | 4,18 |
| Ho | 0,62 | 0,67 | 0,41 | 0,37 | 0,74 | 0,79 |
| Er | 1,79 | 1,80 | 1,20 | 1,05 | 2,09 | 2,24 |
| Tm | 0,27 | 0,26 | 0,18 | 0,15 | 0,30 | 0,32 |
| Yb | 1,81 | 1,62 | 1,29 | 1,02 | 2,05 | 2,19 |
| Lu | 0,28 | 0,24 | 0,20 | 0,16 | 0,32 | 0,34 |

Annexe 8. Trace elements and rare earths in acid lavas, plutonites and sediments

| AGBAOU DEPOSIT | Rhyodacites | Rhyolites | | Gabbros | | Diorites | Metasediments | |
|---|---|---|---|---|---|---|---|---|
| Samples | ARC049D-181 | ARC169D-157 | ARC172D-153 | ADD232-154 | ARC215D-201 | ADD272-252 | ADD355-261 | ARC208D-228 |
| TRACES | | | | | | | | |
| As | <L.D. | <L.D. | <L.D. | 18,64 | 3,09 | 4,68 | 6375,00 | 17,13 |
| Ba | 719,30 | 680,60 | 762,60 | 623,70 | 265,00 | 390,50 | 255,30 | 820,40 |
| Be | 1,13 | 1,56 | 1,58 | 1,11 | <L.D. | <L.D. | <L.D. | 1,75 |
| Bi | 0,13 | <L.D. | 0,26 | 0,11 | 0,12 | <L.D. | 0,95 | 0,18 |
| Cd | <L.D. | <L.D. | <L.D. | <L.D. | 0,16 | <L.D. | 0,32 | <L.D. |
| Co | 4,04 | <L.D. | 1,89 | 41,52 | 32,11 | 41,15 | 50,71 | 13,57 |
| Cr | 62,32 | 41,17 | 84,56 | 65,14 | 452,80 | 589,90 | 114,40 | 58,50 |
| Cs | 1,15 | 1,13 | 0,43 | 13,43 | 6,05 | 8,16 | 1,06 | 0,64 |
| Cu | 8,39 | <L.D. | 15,88 | 73,97 | 53,45 | 55,28 | 102,10 | 29,77 |
| Ga | 18,73 | 19,02 | 18,97 | 17,12 | 15,54 | 13,53 | 17,62 | 17,72 |
| Ge | 0,74 | 0,97 | 0,60 | 1,22 | 1,12 | 1,12 | 0,96 | 1,13 |
| Hf | 2,79 | 1,80 | 2,13 | 3,30 | 4,89 | 2,00 | 3,25 | 3,57 |
| In | <L.D. | <L.D. | <L.D. | <L.D. | <L.D. | <L.D. | <L.D. | <L.D. |
| Mo | 0,57 | 0,44 | 0,81 | 0,86 | <L.D. | <L.D. | 22,81 | 0,61 |
| Nb | 2,42 | 2,38 | 1,18 | 5,44 | 3,46 | 3,87 | 5,87 | 6,33 |
| Ni | 8,70 | <L.D. | 5,01 | 96,19 | 208,00 | 277,10 | 55,88 | 21,54 |
| Pb | 9,07 | 7,55 | 16,18 | 7,82 | 6,27 | 2,46 | 12,49 | 10,52 |
| Rb | 60,66 | 43,54 | 16,76 | 95,46 | 45,66 | 35,81 | 38,12 | 77,03 |
| Sb | <L.D. | <L.D. | <L.D. | 0,21 | 0,41 | 0,73 | 1,01 | <L.D. |
| Sn | 0,85 | 0,70 | 0,95 | 1,31 | 1,17 | 0,96 | 1,33 | 1,77 |
| Sr | 311,20 | 233,60 | 551,70 | 580,90 | 430,30 | 353,40 | 260,10 | 203,10 |
| Ta | 0,60 | 0,45 | 0,47 | 0,63 | 0,37 | 0,37 | 0,58 | 1,00 |
| Th | 4,99 | 4,18 | 2,42 | 3,32 | 6,83 | 2,14 | 4,61 | 3,02 |
| U | 1,99 | 1,97 | 2,31 | 1,04 | 2,25 | 0,69 | 1,48 | 1,08 |
| V | 23,57 | 0,99 | 17,37 | 218,30 | 141,40 | 156,70 | 187,00 | 84,89 |
| W | 5,79 | 0,73 | 1,85 | 0,54 | 2,43 | 0,31 | 7,06 | 2,43 |
| Y | 2,90 | 2,62 | 2,14 | 21,06 | 13,67 | 13,07 | 18,32 | 14,76 |
| Zn | 43,90 | 34,01 | 31,49 | 91,42 | 75,05 | 69,60 | 56,83 | 73,59 |
| Zr | 108,50 | 45,55 | 67,46 | 130,60 | 188,20 | 79,16 | 126,40 | 138,10 |
| RARE EARTHS | | | | | | | | |
| La | 15,57 | 11,41 | 6,23 | 27,33 | 39,64 | 20,67 | 24,19 | 16,78 |
| Ce | 27,51 | 20,28 | 12,97 | 56,93 | 82,36 | 43,97 | 46,98 | 31,84 |
| Pr | 2,91 | 2,17 | 1,63 | 7,04 | 10,20 | 5,58 | 5,35 | 3,70 |
| Nd | 10,45 | 7,87 | 6,80 | 30,90 | 43,78 | 23,51 | 22,30 | 14,67 |
| Sm | 1,74 | 1,34 | 1,43 | 6,13 | 7,64 | 4,43 | 4,66 | 3,08 |
| Eu | 0,54 | 0,34 | 0,42 | 1,71 | 2,01 | 1,28 | 1,39 | 0,80 |
| Gd | 1,19 | 0,92 | 0,98 | 5,00 | 5,01 | 3,33 | 4,05 | 2,77 |
| Tb | 0,14 | 0,11 | 0,11 | 0,70 | 0,60 | 0,46 | 0,59 | 0,43 |
| Dy | 0,63 | 0,52 | 0,45 | 3,86 | 2,83 | 2,43 | 3,34 | 2,51 |
| Ho | 0,10 | 0,08 | 0,07 | 0,73 | 0,47 | 0,45 | 0,63 | 0,50 |
| Er | 0,25 | 0,21 | 0,17 | 2,05 | 1,25 | 1,23 | 1,77 | 1,46 |
| Tm | 0,03 | 0,03 | 0,02 | 0,30 | 0,17 | 0,18 | 0,27 | 0,22 |
| Yb | 0,21 | 0,19 | 0,14 | 2,02 | 1,15 | 1,15 | 1,80 | 1,52 |
| Lu | 0,03 | 0,03 | 0,02 | 0,32 | 0,18 | 0,17 | 0,27 | 0,24 |